

# Optimal PV-EV sizing at solar powered workplace charging stations with smart charging schemes considering self-consumption and self-sufficiency balance

Reza Fachrizal<sup>\*</sup>, Mahmoud Shepero, Magnus Åberg, Joakim Munkhammar

Built Environment Energy Systems Group (BEESG), Division of Civil Engineering and Built Environment, Department of Civil and Industrial Engineering, Uppsala University, P.O. Box 534, SE-751 21 Uppsala, Sweden

## ARTICLE INFO

### Keywords:

Photovoltaic systems  
Electric vehicle charging  
Workplace charging station  
Optimal sizing  
Smart charging  
PV self-consumption

## ABSTRACT

The integration of photovoltaic (PV) systems and electric vehicles (EVs) in the built environment, including at workplaces, has increased significantly in the recent decade and has posed new technical challenges for the power system, such as increased peak loads and component overloading. Several studies show that improved matching between PV generation and EV load through both optimal sizing and operation of PV-EV systems can minimize these challenges. This paper presents an optimal PV-EV sizing framework for workplace solar powered charging stations considering load matching performances. The proposed optimal sizing framework in this study uses a novel score, called self-consumption-sufficiency balance (SCSB), which conveys the balance between self-consumption (SC) and self-sufficiency (SS), based on a similar principle as the F1-score in machine learning. A high SCSB score implies that the system is close to being self-sufficient without exporting or curtailing a large share of local production. The results show that the SCSB performance tends to be higher with a larger combined PV-EV size. In addition to presenting PV-EV optimal sizing at the workplace charging station, this study also assesses a potential SC and SS enhancement with optimal operation through smart charging schemes. The results show that smart charging schemes can significantly improve the load matching performances by up to 42.6 and 40.8 percentage points for SC and SS, respectively. The smart charging scheme will also shift the combined optimal PV-EV sizes. Due to its simplicity and universality, the optimal sizing based on SCSB score proposed in this study can be a benchmark for future studies on optimal sizing of PV-EV system, or distributed generation-load in general.

## 1. Introduction

Since the beginning of the industrial era, the power and transport sectors have been two of the largest sources of greenhouse gas (GHG) emissions, which have been one of the main causes of the global warming [1]. This is due to the fact these two sectors have been mainly relying on fossil fuels [1]. The transition towards more sustainable energy and transportation systems have been promoted globally in the recent years [2]. This has led to a significant growth in the adoption of both renewable energy sources (RESs), such as photovoltaic (PV) systems, and electric transportation, such as electric vehicles (EVs), in the recent decades [3].

However, the integration of both PV and EVs comes with potential technical challenges for the power system due to intermittent generation [4] and increased system load [5]. Furthermore, large scale PV

integration can lead to overgeneration [6], while large scale EV integration can lead to overload [7,8]. These conditions lead to several power system problems such as voltage and frequency deviation and fluctuation [6], component overloading and increased system losses [9]. A costly and time-consuming grid reinforcement will need to be done if such problems are not handled properly [10]. The problems arising from both PV and EV integration can be mitigated by improving the temporal matching between the PV production and EV charging load. Beside mitigating the potential technical problems in the grid, improved PV-EV matching will also lead to economical benefits, such as improved profitability of the PV systems [11], and environmental benefits such as reduced CO<sub>2</sub> emissions, Litjens 2018. For these reasons, many researchers are doing research on this topic [12,13].

<sup>\*</sup> Corresponding author.

E-mail addresses: [reza.fachrizal@angstrom.uu.se](mailto:reza.fachrizal@angstrom.uu.se) (R. Fachrizal), [mahmoud.shepero@angstrom.uu.se](mailto:mahmoud.shepero@angstrom.uu.se) (M. Shepero), [magnus.berg@angstrom.uu.se](mailto:magnus.berg@angstrom.uu.se) (M. Åberg), [joakim.munkhammar@angstrom.uu.se](mailto:joakim.munkhammar@angstrom.uu.se) (J. Munkhammar).

<https://doi.org/10.1016/j.apenergy.2021.118139>

Received 17 August 2021; Received in revised form 15 October 2021; Accepted 26 October 2021

Available online 18 November 2021

0306-2619/© 2021 The Authors. Published by Elsevier Ltd. This is an open access article under the CC BY license (<http://creativecommons.org/licenses/by/4.0/>).

## Nomenclature

### Abbreviations

EV	Electric vehicle
DG	Distributed generation
AC	Alternating current
DC	Direct current
PV	Photovoltaics
SC	Self-consumption
SS	Self-sufficiency
SCSB	Self-consumption-sufficiency balance
EMS	Energy management system
EVCS	Electric vehicle charging station
RES	Renewable energy sources
BESS	Battery energy storage system
V2G	Vehicle-to-grid
DSM	Demand side management
LCOE	Levelized cost of energy

### Variables

$\Delta t$	Temporal resolution (15-min)
$S_{PV}$	PV system size (kWp)
$A$	PV system area (m <sup>2</sup> )
$SoC_{target}$	Targeted state of charge (kWh)
$SoC_{arr}$	State of charge on arrival (kWh)
$P_{PV,t}$	Solar PV generation at time $t$ (W)
$P_{EV,t}$	EV charging load at time $t$ (W)
$P_{EV,max}$	Maximum EV charging rate (W)
$M_t$	Self-consumed power at time $t$ (W)
$\eta_{PV}$	PV cell efficiency (p.u.)
$\phi_{SC}$	Self-consumption (p.u.)
$\phi_{SS}$	Self-sufficiency (p.u.)
$\phi_{SCSB}$	Self-consumption-sufficiency balance (p.u.)
$\eta_{inv}$	PV inverter efficiency (p.u.)
$\eta_{EV}$	EV specific consumption factor (kWh/km)
$\eta_{ch}$	EV charging efficiency (p.u.)
$I_t$	Solar irradiance at time $t$ (W/m <sup>2</sup> )
$I_{STC}$	Solar irradiance at standard test condition (1000 W/m <sup>2</sup> )
$D$	Daily EV driving distance (km)
$E_{EV,day}$	Daily EV charging demand (kWh)
$\mu_{ipark}$	Mean net-load during the parking period (W)
$t_{arr}$	Arrival time (h)
$t_{dep}$	Departure time (h)
$T$	Time steps within the parking period (h)

The PV-EV synergy can be achieved by deploying smart energy management systems (EMS) [13]. Recent studies show that the negative impacts on the low voltage grid from PV and EV can be reduced by the implementation of demand side management (DSM) schemes, such as EV smart charging schemes, both with distributed control [14] and/or with centralized control [15,16]. Consequently, with an improved synergy between PV and EV, the power grid hosting capacity for both PV and EVs can be enhanced as shown in [17] for a case study and in U.K., in [18] for a case study in Sweden, and in [19] for a case study on several test grids. Ref. [20] shows that smart charging schemes can also improve a city scale energy system performance. On

the environmental aspect, a study in [21] shows that an improved PV-EV synergy has a potential to significantly decrease the GHG emission. Beside the technical and environmental advantages, an improved PV-EV synergy potentially adds economic benefits for related stakeholders, such as charging cost reductions for EV owners [22] and increased revenues for PV systems owners and EV aggregators [23].

The potential of PV-EV synergy varies depending on the spatial configuration [24]. At residential buildings, EVs are most commonly parked from evening to morning next day [25]. On the other hand, at workplaces, EVs are most commonly parked from morning to evening within the same day [26]. Thus, the potential PV-EV synergy at the workplace is comparatively higher than at home. With a more promising PV-EV synergy, studies on PV system integration at the workplaces has been common in the recent years, for example in Refs. [27–29].

The temporal load matching for a distributed generation (DG) such as local PV systems is often quantified with self-consumption (SC) and self-sufficiency (SS) measures [30]. A local system with a high SC ratio a high share of local generation self-consumed within the system, regardless of its sufficiency to cover the load. We also have that a local system with a high SS ratio has a high share of the load covered by the local generation, which means that the system relies less on the power grid [31]. This implies that an undersized PV system tends to achieve a higher SC ratio, while an oversized PV system will lead to higher SS. It should be noted that in an undersized PV system, the local generation will contribute very little in covering the load. On the other hand, in an oversized PV system, the majority of the local generation most likely would not be self-consumed and might need to be curtailed, unless the main grid is robust enough to handle the overgeneration [6]. Consequently, besides having an optimal operation via EMS, it becomes important to define the optimal size for PV and EVs in a PV powered electric vehicle charging station (EVCS), or new generation and load in buildings or public facilities in general, so that the local generation is enough to cover the majority of the load without wasting a large share of the generation. Such condition is achieved when both the SC and the SS are high and balanced.

### 1.1. Related work and motivation

Integration of PV and EVs in the built environment has been a major topic within the power and energy system research field in the recent years. This includes PV-EV integration at workplaces. A considerable number of studies on EV integration at workplaces with different focuses has been carried out. For example, in [32], the impact of EV charging demand on distribution transformers in an office area was assessed. A system design for solar powered EVCS at workplaces with a case study in the Netherlands was presented in [28]. In [33], integration of EVs in an office building located in southern Italy to increase PV SC was studied. Recent research in [34] studied the effectiveness of an off-grid solar powered charging system at long-term parking locations.

The EV integration studies are often extended to system performance enhancements utilizing the flexibility of the EVs, e.g., with smart charging and vehicle-to-grid (V2G) schemes. In [35], a smart charging architecture for PV powered EVCS based on DC voltage sensing was proposed. The smart charging objective of the mentioned work was to increase PV utilization and avoid charging during the peak load periods. A smart charging scheme to increase solar-to-vehicle (S2V) ratio with a case study of a charging station in a university was presented in [27]. In [36], a real time smart charging scheme involving PV generation for an EVCS at workplace area was proposed. The objective of the smart charging in that paper was to minimize the charging cost. Ref. [29] presented a smart charging scheme based on PV forecast at the workplace, also with an objective of charging cost minimization. Smart charging and V2G schemes at EVCS equipped with a PV-battery energy storage system (BESS) also with a cost minimization objective was proposed in [37]. Ref. [38] presented a charging management

strategy for portable charging stations in EV charging networks in Washington, U.S. in order to reduce both peak loads and charging queue time. A charging management strategy for large scale fast charging stations to avoid under-voltage problems in the medium voltage grid was recently proposed in [16]. The charging management scheme in the mentioned study used an algorithm called pre-centralized voltage regulation. In [39], a cyber-physical co-modeling of a real world system simulating smart V2G schemes was conducted. The objective of the mentioned study was load flattening and PV utilization. A deep reinforcement learning method for EV smart charging in the presence of PV generation was used in a recent research in [40]. The control objective of the smart charging scheme in the mentioned paper was to increase the PV utilization.

Considerable amounts of previous research also studied the optimal sizing of PV in different parts of the built environment. The recent trend shows that the optimal sizing of PV systems is often assessed together with BESS sizing. Ref. [41] presented a framework to define the optimal PV-BESS sizing in residential buildings considering techno-economic aspects, i.e., SC and frequency regulation participation. This approach was also later used in another study on optimal household PV-BESS sizing in [42]. In [43], the optimal PV sizing and operation in a residential building which also includes household load, EV charging load, BESS was presented. The approach in the mentioned paper was also based on techno-economic aspects. The cost-optimal PV-BESS sizing in an EVCS was studied in [44] considering a dynamic electricity pricing and in [45] considering stochastic nature of both PV generation and EV charging behavior. Ref. [46] presented optimal PV-BESS sizing considering the implementation of a smart EMS with the objective to cover residential EVCS loads.

The studies on the optimal EVCS sizing in terms of the number of charging ports is comparatively more scarce than studies on PV-BESS sizing. An example of such studies is [47], where an optimal EVCS sizes powered by commercial PV systems considering reactive power support was determined. Ref. [48] also presented a study on EVCS optimal sizing in terms of the number of charging ports together with the integrated PV-BESS sizing considering economic aspects. In [49], a dynamic approach for cost-optimal planning for EVCS construction, which includes optimal capacity of the EVCS, was proposed. The integration of rooftop PV system was also included in the mentioned study. Recently, Ref. [50] proposed an optimal sizing method of EVCS in cities considering urban traffic flow. An extensive urban study and traffic flow simulations were used to define the optimal sizing of the EVCS.

As reviewed, the economic aspects have been the most common considerations in defining the optimal system size of solar powered buildings or infrastructures in the previous studies. Even though the economic aspect is a big interest for the building/infrastructure owners, economic aspects in defining the optimal PV size will be subject to local policies and regulations [51]. The local policies and regulations related to PV, which are likely to be different between regions and countries, are including but not limited to levelized cost of energy (LCOE), feed in tariffs, tax and subsidy related to RES and CO<sub>2</sub> emissions [52]. Thus, different case studies will likely require different formulation for cost optimal sizing.

In comparison to the economic aspects, the formulation of SC and SS are universal for any local RES powered buildings or infrastructure as shown in several studies, for example in [30,53,54]. Thus, optimal sizing framework based on these parameters has the potential to become a universal benchmark. To the best knowledge of the authors, there has not been any study which proposed a framework which consider the balance between SC and SS for optimal PV-EV sizing at an EVCS or for optimal PV-load sizing in general, and that can be considered a research gap. Furthermore, the impact of smart charging schemes to such optimal PV-EV sizing in the workplace EVCS has not been conducted previously.

The balance between SC and SS is important because as discussed earlier, an oversized DG will lead to a low SC despite the high SS

achieved. On the other hand, an undersized DG will lead to a low SS despite the high SC achieved. In order to achieve an optimal DG utilization, a novel measure combining both SC and SS measures are needed. Several references, e.g., [55–57], have previously presented a measure combining both SC and SS, albeit there only for load matching assessment purposes, and not for PV-load sizing purposes. However, this measure did not represent accurately the actual load matching performance for buildings with lower middle SC and SS performance. A measure combining the SC and SS that accurately represent the load matching performance is another research gap. A novel formulation combining SC and SS in order to quantify the performance of PV powered buildings/infrastructures in a more representative way is proposed in this study. The measure is also used to define the optimal PV-EV size in the workplace charging stations. The comparison between the previous measures and the novel measure proposed in this study is discussed comprehensively in Section 3.2.

## 1.2. Aims and structure of the paper

This paper aims to complement previous research by proposing an optimal PV-EV sizing framework considering the balance between SC and SS as well as assessing the optimal operation for EVCS with smart charging schemes with an objective of flattening the net-load profile. The framework is tested on Swedish conditions for travel behavior and solar irradiance. In addition, it is also tested for irradiance on Oahu, Hawaii, to determine the effect of the modeling with two different climatic regions on the results. The following topics are investigated:

1. The potential of improved synergy between PV generation and EV charging in the workplace charging station by smart charging schemes quantified by SC and SS measures.
2. The optimal PV-EV sizing for the workplace charging station using a novel framework and measure which considers the balance between SC and SS.
3. The impact of the deployment of EV smart charging schemes to the optimal PV-EV sizing for the workplace charging station.
4. The sensitivity analysis of optimal PV-EV sizing and operation for the workplace charging station in different climatic regions to test the universality of the proposed framework.

This paper is organized as follows: Section 2 presents the simulation data, assumptions, scenarios, EV charging schemes used in this study as well as the load matching measures and the framework proposed in this study. Section 3 presents the results for generation-load profiles, load matching performance enhancement by the smart charging schemes, optimal PV-EV sizing in the workplace charging station and sensitivity analysis of the models and the framework with different irradiance profiles. In Section 4, the highlights of the results and possible future work are discussed. Section 5 presents the main conclusions of the paper.

## 2. Methods

This section describes the methods used in the study. Fig. 1 shows a flowchart depicting the workflow of the conducted studies in this paper. The details of data, the case study, models, scenarios, assumptions used in this paper as well as the load matching measures and the framework proposed in this paper are further described in Sections 2.1–2.4. In this paper, the simulations are based on the conditions for Sweden, with a wide applicability for high latitude regions. Other than that, this paper also utilized Hawaii solar irradiance profile for sensitivity analysis of the models in lower latitude climatic regions.

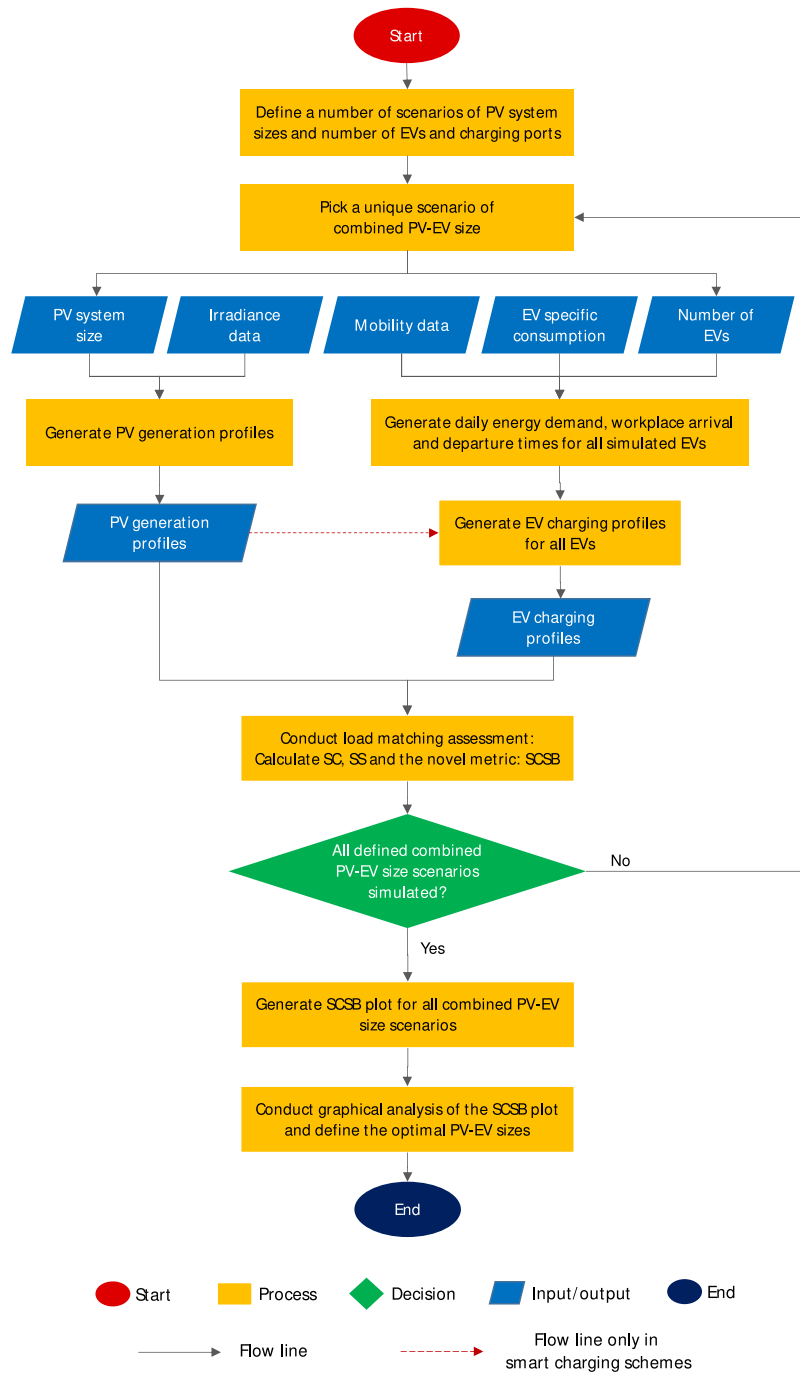


Fig. 1. Flowchart of the conducted studies in this paper.

## 2.1. Data and case study

### 2.1.1. Solar PV power production

The solar power production profiles for the Swedish conditions in this study are based on a synthetic yearly irradiation profile in Stockholm, Sweden, with latitude 59.3° N and longitude 18.0° E from Meteornorm [58]. The simulated PV system at Stockholm site was tilted 42° to the south to maximize the yearly energy yield. Apart from Stockholm profile, this study also utilized global horizontal irradiance (GHI) data for Oahu, Hawaii, USA, from Oahu Solar Measurement Grid with latitude 21.3° N and longitude 158.1° W [59].

Commonly, the PV generation at time  $t$ ,  $P_{PV,t}$  (W), can be written as [60]

$$P_{PV,t} = \eta_{inv} \times \eta_{PV} \times A \times I_t, \tag{1}$$

where  $\eta_{inv}$  is the inverter efficiency which in this study was set to 0.95,  $\eta_{PV}$  is the PV cell efficiency,  $A$  is the PV area ( $m^2$ ), and  $I_t$  is the incident solar radiation on the tilted place ( $W/m^2$ ) at time  $t$ . For the simulations in this study, PV system size in kWp is of interest rather than the PV area. The PV system size in kWp for this study referred to one of the silicon-based PV system offered in the Swedish market, with  $\eta_{PV}$  of 0.167 [61]. In the referred system, 1 kWp system will have a PV area of 6  $m^2$ .

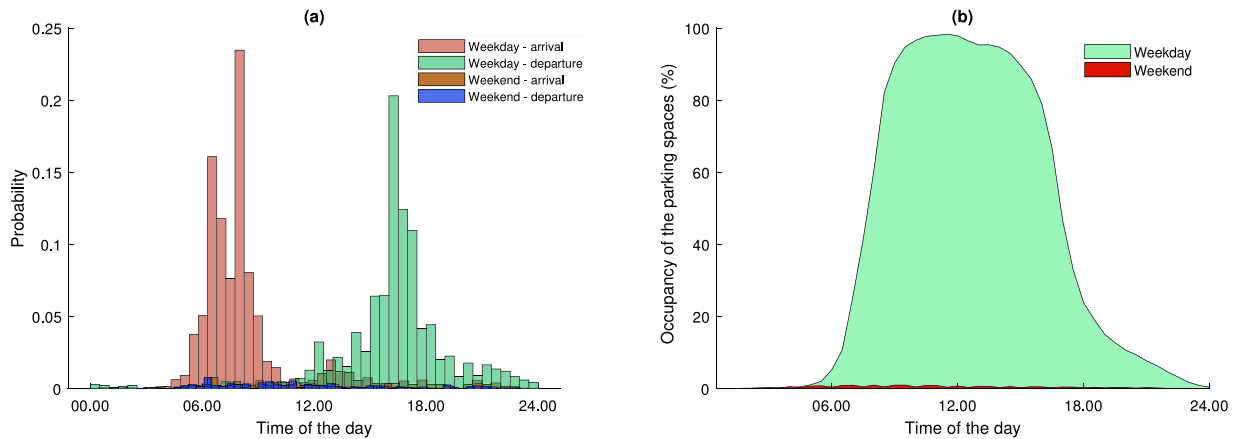


Fig. 2. EV user workplace mobility statistics for this study: (a) time arrival at and departure from the workplace and (b) mean daily occupancy of workplace parking spaces for weekdays and weekends.

### 2.1.2. Mobility patterns and daily charging demands

This study utilized Swedish travel survey data in 2006 obtained from [62] to model user mobility patterns and the EV charging demands. This approach is motivated by the finding in [25], which showed and validated that modeling the EV charging demand based on mobility and travel survey data is an appropriate way to resemble the real EV charging demand. The arrival and departure times, the origin and destination locations, and the distance traveled in each trip were available in the used survey data. In this study, home to work mobility patterns were used to define the arrival times at the workplace, while work to home mobility patterns were used for the departure times. It should be noted that the home-work-home mobility patterns, both in histogram shapes and magnitudes, are different between weekdays and weekends, as illustrated in Fig. 2. Based on the data used in this study, only around 7% of the users go to office on the weekend and with irregular and shorter parking periods. From this survey data, the user mobility patterns were generated with a Monte Carlo sampling method. Fig. 2(a) and (b) shows the histogram of users' workplace arrival and departure times, and the mean daily fraction of the vehicles at the workplace parking lot respectively. From Fig. 2, it can be seen that most of the cars arrive at the workplace between 06.00 and 10.00 and leave from the workplace between 15.00 and 18.00. This results in a very high parking lot occupancy during the day.

The daily EV energy use was also modeled with a Monte Carlo method by randomly sampling the distance traveled for home to work trips from the survey data [62]. According to [60], the daily EV energy demand for charging can be defined as

$$E_{EV,day} = \eta_{EV} \times D, \quad (2)$$

where  $D$  is the daily driving distance, and  $\eta_{EV}$  is the EVs specific consumption (kWh/km). In this study,  $\eta_{EV}$  is subjected to the air temperature condition to represent the seasonal EV energy needs as EVs require more energy for passengers' comfort heating in colder weather. The daily average temperature over the year was taken into account to define  $\eta_{EV}$  in each day of the year. The  $\eta_{EV}$  was set to 0.25 kWh/km on a day with a mean daily temperature of  $-10^{\circ}\text{C}$ , which was the day with the lowest mean daily temperature in this data set. On days without the need for a comfort heating system on, which was assumed to be the days with mean daily temperature higher than  $10^{\circ}\text{C}$ ,  $\eta_{EV}$  was set to 0.15 kWh/km. The  $\eta_{EV}$ s on other days were set between 0.15–0.25 kWh/km depending on the mean daily temperature in those days. The mean daily temperature for Stockholm was obtained from the Swedish Meteorological and Hydrological Institute (SMHI) [63]. For the case study in Hawaii, the  $\eta_{EV}$  was set to 0.20 kWh/km all the year [64]. This is in order to represent the cooling needs for vehicle thermal comfort in warm Hawaii climate [64].

In this study, the maximum usable energy in the battery is set to 30 kWh. This is assuming that the battery can provide enough energy for the daily trips within a city. The daily driving distance  $D$  is calculated by doubling the randomly sampled home-workplace trip distance. The assumption is that each EV performs two equally long trips a day, such as a trip from work to home and back to work again in the next morning. It should be noted that in this case, it is assumed that EV only charge once in a day and in the workplace charging station to fulfill its daily energy demand. The motivation behind this is to have best-case approximation of the workplace EVCS utilization.

The maximum charging power was set to 11 kW, which is a common power rating for AC chargers at public charging stations [65]. In this study, it is worth mentioning that the schemes do not require a fast charging with high charging power for at least two reasons. First, most of the EVs stay parked for a long period, i.e., during working hours, thus the EV energy demand can still be fulfilled with slow charging. Second, the utilization of the local PV system integrated at the EVCS will be higher with slow charging. In this study, the charging efficiency was set to 90%, which referred to the average of Level 2 charging efficiency [66]. Additionally, it was assumed that the charging efficiency was constant regardless of the charging power.

## 2.2. EV charging schemes

This section describes the uncontrolled charging, the distributed smart charging and the centralized smart charging schemes simulated in this study. The simulated smart charging schemes were based on the residential EV smart charging schemes presented in [67], with some required modifications to represent the workplace EVCS condition. In this study, as a major assumption, the model for smart charging does not alter the mobility patterns of the driver.

### 2.2.1. Uncontrolled charging

In the uncontrolled charging scheme, EVs charge opportunistically. This implies that EVs start charging with the maximum charging power (11 kW) as soon as they are parked at the workplace. The scheme does not consider surrounding parameters, e.g., local PV generation or electricity price. The charging is stopped when the targeted SoC is met, which corresponds to a full charge of usable battery capacity (30 kWh). If the parking duration is not long enough to make the EV fully charged, the charging is stopped at the departure time. From this scheme, a full year time-series of uncontrolled EV charging load was generated for this study.

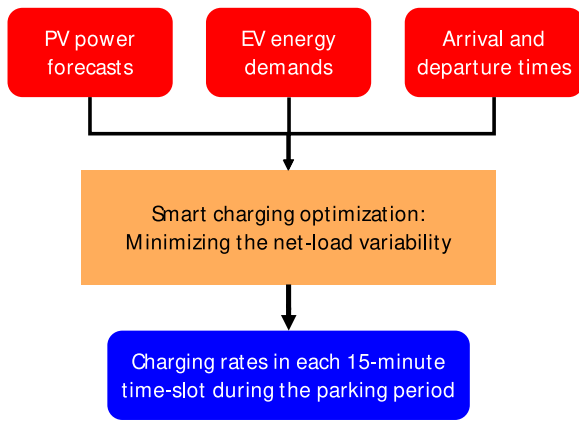


Fig. 3. Overview of the smart charging scheme in this study.

### 2.2.2. Smart charging

The smart charging scheme in this study is adapted from [67]. In the smart charging scheme, the charging does not always start immediately upon arrival at the workplace and nor does it always use the maximum charging power. The charging scheme considers a PV production forecast within the parking period. The smart charging scheme in the mentioned paper has an objective of minimizing the residential building net-load variability with constraints of targeted state of charge (SoC) and maximum charging rate. In this study, no residential nor office building load was considered, since the main objective of installing PV system is to cover the EV charging load in the EVCS. Thus, only net-load between EV load and PV generation is considered. Minimizing the net-load variability will lead to a flatter net-load profile, which will consequently increase the local generation SC and decrease the peak loads. Fig. 3 shows an overview of the proposed smart charging scheme. It should be noted that the perfect forecasts of PV generation were used for the smart charging simulations in this study, since one of the objectives of this study was to define the highest possible PV-EV load matching potential at workplaces using the smart charging schemes. The objective function of the smart charging is represented by a population variance equation, which is expressed as

$$\min \sum_{t \in T} (P_{EV,t} - P_{PV,t} - \mu_{tpark})^2. \quad (3)$$

The denominator part of the variance equation, which is a constant, is not taken into account in the objective function as it will not change the optimization result. The constraints of the optimization are defined as

$$\begin{aligned} \text{s.t. } \eta_{ch} \sum_{t \in T} P_{EV,t} \Delta t &= SoC_{target} - SoC_{arr}, \\ 0 &\leq P_{EV,t} \leq P_{EV,max}, \quad \forall t \in T. \end{aligned} \quad (4)$$

where  $T$  is the time steps within the parking period from arrival time  $t_{arr}$  and departure time  $t_{dep}$  of the car,  $P_{EV,t}$  is the charging power rate at time  $t$ ,  $P_{PV,t}$  is the solar power production at time  $t$ ,  $\mu_{tpark}$  is the mean net-load during the parking period considering the EV charging load. In the constraint,  $\eta_{ch}$  is the charging efficiency,  $SoC_{target}$  is the state of charge targeted in the battery in kWh,  $SoC_{arr}$  is the state of charge in the battery on arrival in kWh, and  $P_{EV,max}$  is the maximum charging power rate. The mean net-load during the parking period  $\mu_{tpark}$  is defined as

$$\mu_{tpark} = \frac{(SoC_{target} - SoC_{arr}) / \eta_{ch} - \sum_{t \in T} P_{PV,t} \cdot \Delta t}{t_{dep} - t_{arr}}. \quad (5)$$

With this formulation, the scheme will attempt to make the net-load at each time step to be as close as possible to value of  $\mu_{tpark}$ , resulting a maximally flat net-load profile. Since the formulation has a quadratic

objective function, a quadratic programming approach was needed for this charging optimization.

Both distributed and centralized smart charging were simulated in this study. The formulations of distributed and centralized charging schemes in this study are essentially the same, as was studied for residential-charging in [67]. The only differences between the schemes are the coordination scopes and the share of PV generation considered for the optimization input. In the distributed smart charging, the control in each port is conducted considering only the individual EV. The other EVs in the EVCS are not considered. In addition the PV generation input to the optimization formulation is scaled down based on the number of EV charging ports. For example, in an EVCS with  $n$  charging ports, each charging port will only consider  $1/n$  of the total generated power from the whole installed PV systems at the EVCS. This strategy is needed for the particular smart charging scheme to avoid the avalanche effect, where all EVs charge simultaneously during the peak of PV generation without coordination [68]. The avalanche effect can lead to a new high net-load in the solar peak hours, while the PV generation in other hours will not be well-utilized [69].

In the centralized charging, the coordination scope is for the whole EVCS and with all the PV generation in the EVCS considered for the optimization input. The difference between the distributed and the centralized charging schemes is illustrated in Fig. 4. There are some additional rules in the presented centralized smart charging scheme to avoid avalanche effect. The first one is that, if more than one EVs arrive at time step  $t$ , the charging scheduling of the EV that will depart earlier will be executed earlier since the EVs which park longer have a higher flexibility to make the total net-load profile flatter. The second one is that the forecast of PV net-generation in the scheduled horizon is always updated after a charging schedule of an EV is defined. The update of PV net-generation forecast is defined as

$$P_{PV,t} = P'_{PV,t} - P_{EV,t}, \quad (6)$$

where  $P'_{PV,t}$  is the perfect forecast of PV net-generation at time  $t$  before the latest EV scheduling is defined. With this update, the next EV charging scheduling considers the change of PV net-generation profile due to the allocation for the previously scheduled EV charging load.

### 2.3. Load matching measures and framework

This section describes SC and SS measures which are two of the most common load matching indicators for PV systems integrated in buildings or public facilities [30]. In addition, the score on the balance between SC and SS is proposed here. Fig. 5 shows a schematic outline of workplace EVCS daily electricity net-demand represented by area A and PV net-generation represented by area B. The overlapping part in area C is the PV electricity directly utilized within the EVCS. SC is defined as the fraction of the self-consumed PV electricity to the total PV electricity production, while SS is defined as the fraction of self-consumed PV electricity to the total PV electricity production. Based on the illustration in Fig. 5, SC and SS can be defined as [30]

$$SC = \frac{C}{B+C}, \quad (7)$$

$$SS = \frac{C}{A+C}. \quad (8)$$

For the case of PV power used for EV charging only, the self consumed power at time  $t$ , can be defined as [30]

$$M_t = \min(P_{EV,t}, P_{PV,t}). \quad (9)$$

Also, it can be shown that the SC and SS can be defined mathematically as [30]

$$\phi_{SC} = \frac{\int M_t dt}{\int P_{PV,t} dt}, \quad (10)$$

$$\phi_{SS} = \frac{\int M_t dt}{\int P_{EV,t} dt}. \quad (11)$$

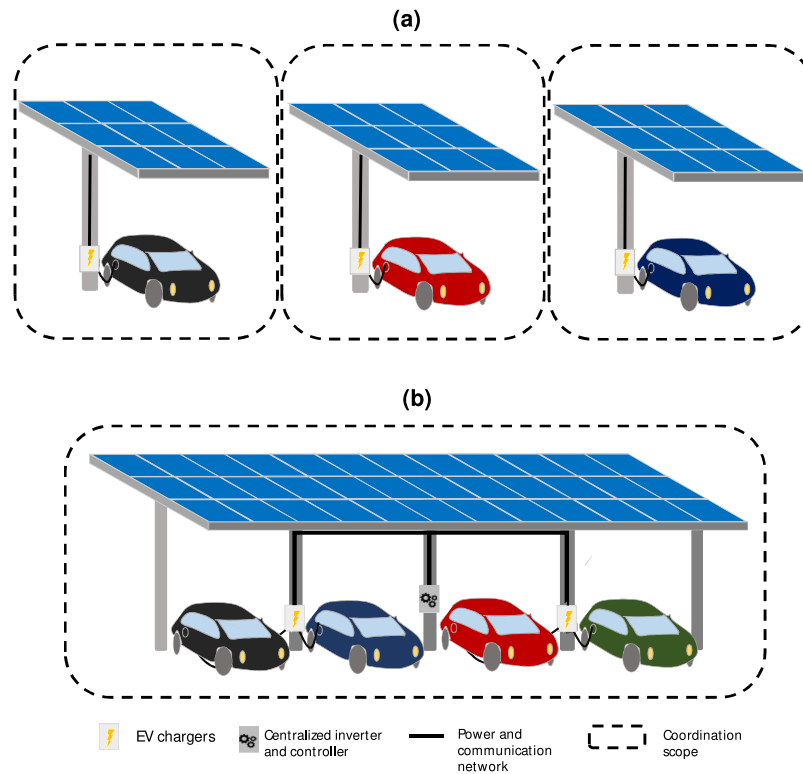


Fig. 4. The architecture of (a) distributed and (b) centralized smart charging.

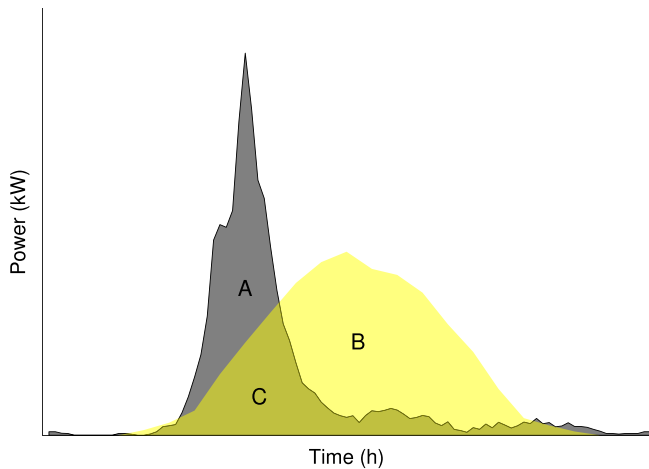


Fig. 5. Schematic outline of daily EV charging load (A + C), PV generation (B + C), self-consumed electricity (C) for the workplace charging.

A high SC means that a large share of the PV electricity is self-consumed to supply the load. A high SS means that the load is mostly supplied from the locally produced PV electricity.

As mentioned earlier, an undersized PV system tends to achieve a higher SC ratio, yet the contribution of the PV system will be too small in covering the load. On the other hand, an oversized PV system lead to higher SS, yet a large share of the local generation most likely would not be self-consumed and in most common scenarios should be curtailed, except if the power grid is robust enough to deal with the surplus generation [6]. Thus, SC alone or SS alone will barely represent how well the PV-load synergy. In fact, increasing the PV size to increase SS will lower SC in cases without BESS and/or EMS. Therefore, both measures should be taken into account when assessing the performance of a local PV system integrated in buildings or infrastructures.

Table 1

Comparison of SC, SS and SCSB of three example systems with the same arithmetic mean of SC and SS: 0.5.

Case	SC	SS	SCSB
a	0.80	0.20	0.32
b	0.50	0.50	0.50
c	0.20	0.80	0.32

In order to have a viable score that combines SC and SS, we introduce a novel metric called self-consumption-sufficiency balance (SCSB), which is defined as

$$\phi_{SCSB} = \frac{2\phi_{SC}\phi_{SS}}{\phi_{SC} + \phi_{SS}} \tag{12}$$

The score is intended to convey the balance between the SC and SS by combining the two measures in a single metric. The SCSB score is based on harmonic mean formula which is one of the Pythagorean means along with arithmetic and geometric means [70].

The SCSB score ranges between 0 and 1. A high SCSB score can only be achieved if both the SC and the SS are high. The SCSB scores for different SC and SS values are illustrated in Fig. 6. The score gives a low score if either of the SC or the SS is too low, regardless of the high value of the other parameter. In Fig. 6 and Table 1, three example cases system: a, b, c, are compared. The three cases have the same SC-SS arithmetic mean of 0.5. However the SCSB scores of case a and c are lower than the score of case b. This is because the SC and SS in case b are balanced. On the other hand, in case a, the SS is significantly lower than the SC indicating an undersized PV system, and in case c, the SC is significantly lower than the SS indication an oversized PV system. In conclusion, the SCSB score will reward the balance between SC and SS instead of a very high value of one of the parameters if the other parameter is too low.

Other measures combining both SC and SS measures in a single measure have been presented in [55] as Behavior Ratio and in [56,57] as Renewable Energy Use, albeit there only for building performance

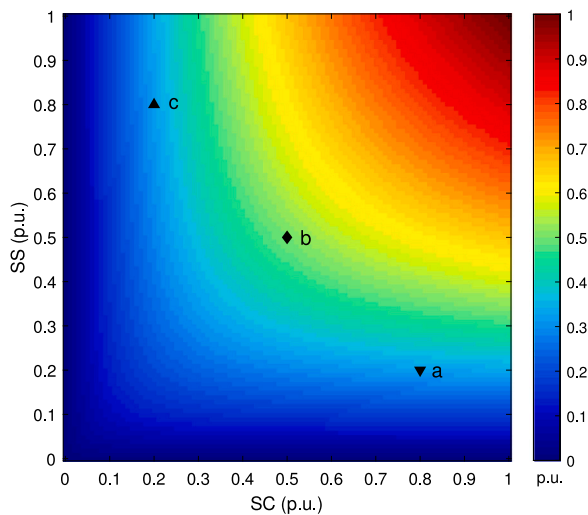


Fig. 6. SCSB scores for different SC and SS values. Point a, b and c are three example cases where the arithmetic mean of SC and SS is 0.5.

assessment purposes, and not for PV-load sizing purposes. In both of those measures, the annual SC is multiplied by the annual SS. Similarly to the SCSB score proposed here, those measures range between 0 and 1, and the perfect score of 1 can be achieved if both of the SC and the SS are 1. The *Behavior Ratio/Renewable Energy Use* scores for different SC and SS values are illustrated in Fig. 7(a). From Fig. 7(a), it can be seen that those measures will give a significantly lower score for lower middle SC and SS performances. For instance, in the example cases presented in table Table 1, both of those measures will give case a, b and c a score of 0.16, 0.25 and 0.16, respectively, while both the actual SC and SS are significantly higher. Thus, those measures did not represent accurately the actual load matching performance for buildings with lower middle SC and SS performance.

The square root of *Behavior Ratio/Renewable Energy Use* score is the geometric mean of the SC and the SS, and can represent the actual load matching performance more accurately than *Behavior Ratio/Renewable Energy Use*. The geometric means for different SC and SS values are illustrated in Fig. 7(b), and it can be seen the pattern has a high similarity with the proposed SCSB score pattern using the harmonic mean. However, we opted to choose the harmonic mean over the geometric mean because, among the pythagorean means, the harmonic mean is an appropriate mean score for the data in which the values are rates or ratios [70,71], like the SC and the SS.

Other than that, a similar principle using harmonic mean is already proven to be useful in other field, i.e., machine learning, for a similar problem. In the machine learning field, the principle using harmonic mean is used for an important score, specifically for classification problems, called F1-score or F-score [71]. The F1-score is intended to convey the balance between two important parameters: precision and recall [71]. Like SC and SS, both precision and recall are ratios. The F1-score is primarily used to compare the overall performance of two or more classification models and can help to define the most suitable model for a certain classification problem. [71]. Similarly, using SCSB score to assess the load matching performance can be a framework that helps to define the suitable system size of a certain RES powered building or infrastructure, such as PV powered EVCS.

#### 2.4. Simulation scenarios

In order to investigate the scores for a wide variety of scenarios, several scenarios on the number of EV charging ports were simulated, i.e., 5, 10, 20, 40, 60, 80 and 100. Similarly for the PV sizes, several scenarios were simulated, they are: 5 kWp, 10 kWp, 20 kWp, 40 kWp,

60 kWp, 80 kWp and 100 kWp which corresponding to 30 m<sup>2</sup>, 60 m<sup>2</sup>, 120 m<sup>2</sup>, 240 m<sup>2</sup>, 360 m<sup>2</sup>, 480 m<sup>2</sup> and 600 m<sup>2</sup>, respectively.

Beside the scenarios from the combination between PV and EV sizes, three charging scenarios were simulated: uncontrolled charging, distributed smart charging and centralized smart charging. These three scenarios were also simulated in a sensitivity analysis where Hawaiian irradiation data was used. The sensitivity analysis aims to test the framework for a different climate zone with different irradiation profiles.

### 3. Results

#### 3.1. Generation-load profiles

Fig. 8 shows the PV power production and EV charging load profiles with different charging schemes at the charging station for the Stockholm case in three different weeks, i.e., a full-week in each of March, June and December. These months were chosen to cover a wide variety of seasons. The mean daily generation-load profile in March, June and December are shown in Fig. 9. In both figures, the size of the PV system was 40 kWp and the number of charging ports was set to 40. The generation and load profiles in March, June and December represents the profiles in the days with average, longest and shortest daylight hours in Sweden respectively. This is intended to show the generation-load profile variability among seasons. By visual inspection of Figs. 8 and 9, it can be seen that the uncontrolled charging profile can be easily distinguishable from the smart charging profiles. The uncontrolled charging load profile has daily peaks between 08.00–10.00, while the smart charging load profiles have daily peaks between 12.00–13.00 following the solar generation diurnal patterns. As a result, the temporal matching between the PV generation and smart charging loads are significantly higher compared to the one between PV generation and uncontrolled charging load. The distributed smart charging load profile is similar to the centralized smart charging load profile. The only difference between the two is that the centralized smart charging was slightly flatter, while the distributed smart charging profile has more ripples since the charging was not coordinated by single central unit.

By comparing each subfigure in Figs. 8 and 9, the seasonality of the PV generation can be observed. With this particular case of combined PV-EV size, the PV contribution for EV charging in December is very low, even with smart charging schemes. However, the smart charging schemes in winter still gave important advantages by avoiding high peak charging load and making the load profile flatter. On the other hand, in June, there was more PV electricity generated than EV charging energy demand. With perfect forecast smart charging schemes, there would still be electricity surplus at the EVCS in June. This seasonal variability would be a limitation for reaching a perfect load matching on annual basis.

Beside PV seasonality, the user mobility behavior from and to the workplace would also be a limitation to the load matching potential. As can be seen in Fig. 8, the charging load on weekends was significantly lower than on weekdays, since only a very few users visited the workplace on weekends. However, it should be noted that the assumption in this study was that the EVCS was strictly for workplaces only, with workplace mobility patterns. Other parts of the built environment combining residential, workplace and commercial buildings such as malls, are expected to have different weekday and weekend charging profiles.

#### 3.2. Load matching performances

In this section, the results in load matching performances, i.e., SC, SS and SCSB, from this study is presented. Fig. 10 shows the load matching performances for the Stockholm case, i.e., (a) SC, (b) SS and (c) SCSB, in some combined PV-EV size examples simulated in this

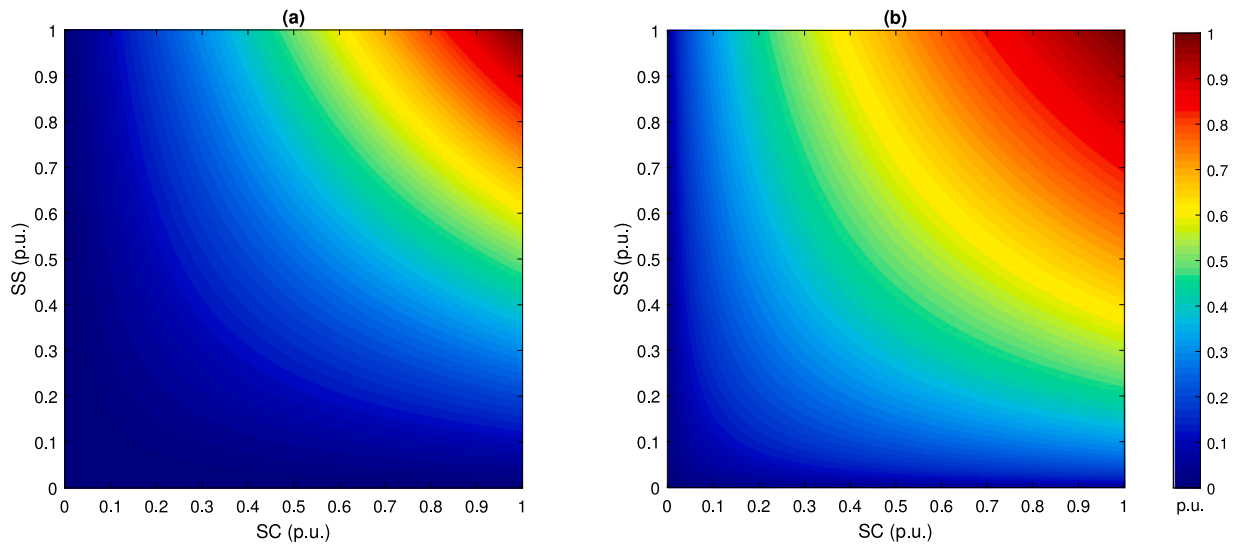


Fig. 7. (a) Behavior Ratio [55] or Renewable Energy Use [56] scores and (b) geometric means of SC and SS for different SC and SS values.

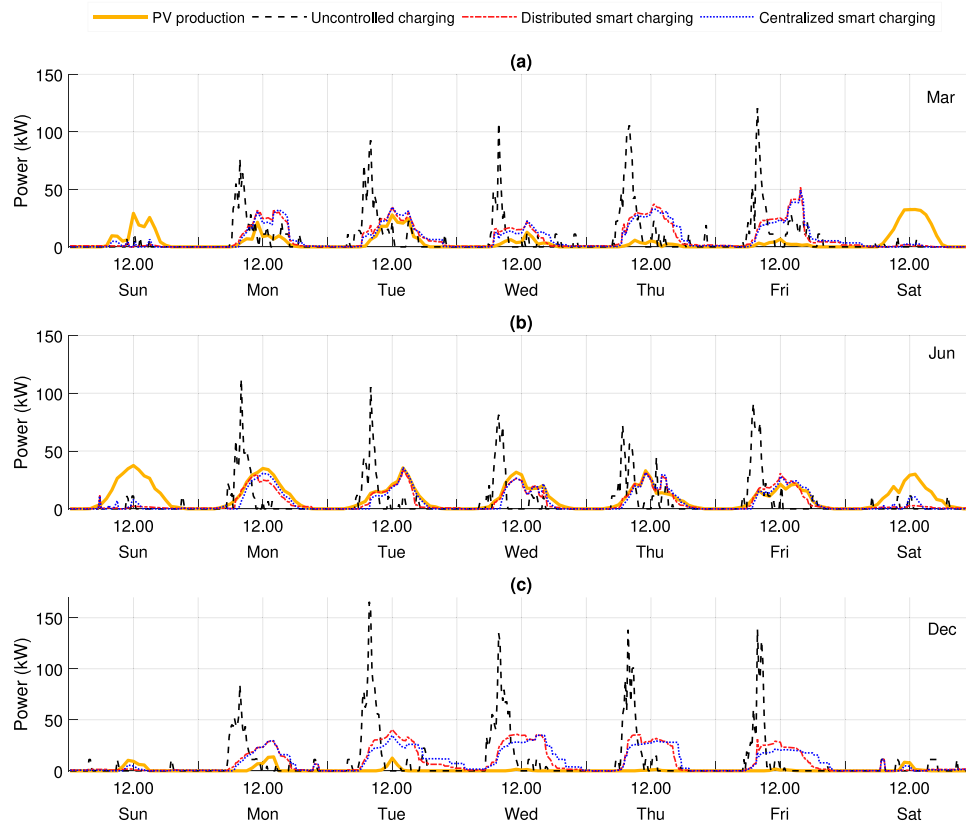


Fig. 8. Example of PV power production and EV charging load profiles with different charging schemes at the charging station with 40 kWp PV system and 40 charging ports in the third full-week of (a) March, (b) June and (c) December: Stockholm case.

study. In the figure, black lines represent scenarios with uncontrolled charging, red lines represent scenarios with distributed smart charging and blue lines represent scenarios with centralized smart charging. Dotted lines represent scenarios with 20 chargers, dashed lines represent scenarios with 40 chargers and solid lines represent scenarios with 60 chargers. By comparing the results, it can be seen that the smart charging improved SC and SS regardless of the combined PV-EV sizes. The exact numerical estimates of the improvements in the SC and the SS are presented in Section 3.2.1.

From Fig. 10, it can also be seen by comparing the results for different combined PV-EV sizes, that the SC was lower when the PV size was higher and the number of EV charger ports was lower. On the other hand, the SS was higher for the same reasons. Unlike the SC and SS with consistent trends when the PV and EV sizes were increased or decreased, the SCSB plots are concave-shaped which implies that the maximum is neither obtained from the lowest nor the highest value of the independent variable. Because of the concavity of the SCSB curve, it allows for finding an optimal configuration of number of EV charging ports and PV size. For example, based on Fig. 10(c), the maximum SCSB

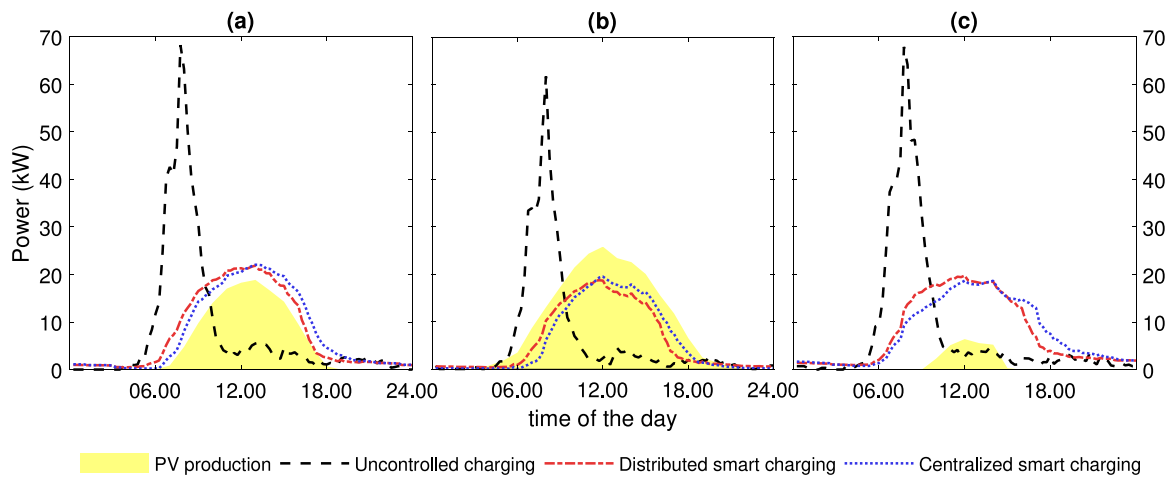


Fig. 9. Daily average of PV power production and EV charging load profiles with different charging schemes at the charging station with 40 kWp PV system and 40 charging ports in (a) March, (b) June and (c) December: Stockholm case.

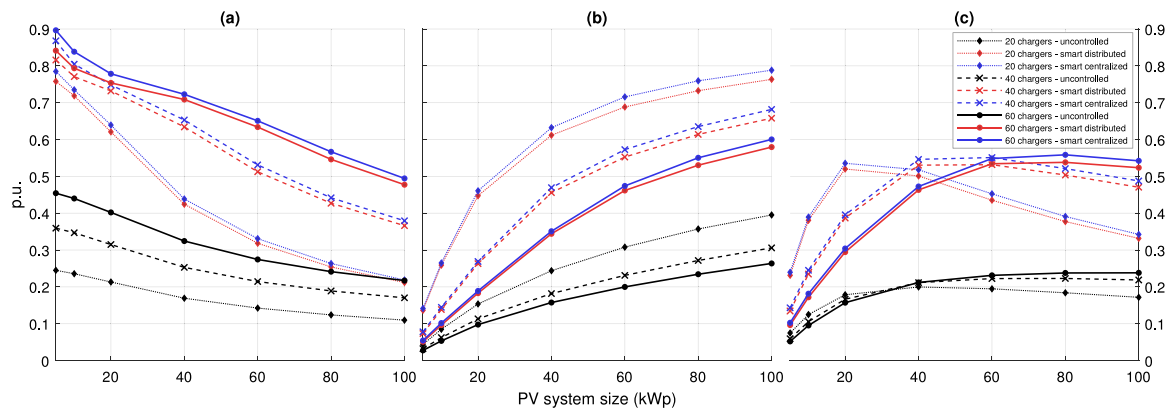


Fig. 10. (a) SC, (b) SS and (c) SCSB in the workplace charging station for selected PV sizes and numbers of EV charging ports: Stockholm case.

for an EVCS with 20 charging ports with smart charging capability is obtained when the PV system size is 20 kWp. A more comprehensive presentation and analysis on configuration of number of EVs and PV system size based on the SCSB metric is presented in Section 3.3.

As discussed earlier, the solar seasonality affects the temporal matching between the PV and the load in different seasons. This led to varying SC and SS at different times of the year. Fig. 11 shows the SC, SS and SCSB at the EVCS with a 40 kWp PV system and 40 EV charging ports in different months of the year. In the figure, it can be seen that the SC was higher during the winter where the generation was low while the SS was higher during the summer where the generation was high. The SCSB, as the harmonic mean, was higher during the summer compared to during the winter. This was due to an extremely low SS during the winter. As mentioned earlier, the annual PV load matching at high latitude will be limited by its high solar seasonality, unless seasonal storage systems which can store electricity in the summer and dispatch it in the winter are deployed, which is not investigated in this study.

### 3.2.1. Performance enhancements with smart charging

Tables 2 and 3 show the SC and SS improvements, respectively, in the distributed and centralized smart charging scenarios compared to the ones in the uncontrolled charging scheme in different combined PV-EV configurations at the EVCS for the Stockholm case. The improvements were quantified in percentage point increase. It should be noted that the smart charging schemes with the perfect forecast simulated in this study will be a best-case approximation for SC and SS scores using the schemes.

Table 2

SC increases in percentage points at the EVCS with varying combined PV-EV sizes with distributed charging (D) and centralized charging (C) compared to uncontrolled charging with a maximum charging power of 11 kW: Stockholm case.

PV system size (kWp)	Number of EV charging ports									
	20		40		60		80		100	
	D	C	D	C	D	C	D	C	D	C
20	40.8	42.6	41.7	43.3	35.2	37.6	30.7	34.2	26.1	30.2
40	25.5	26.9	38.1	40.0	38.4	39.8	35.4	36.9	31.6	33.4
60	17.6	18.9	29.8	31.7	35.9	37.6	37.5	38.7	35.6	36.7
80	13.0	13.9	23.8	25.3	30.5	32.5	35.3	36.8	36.7	37.9
100	10.2	10.9	19.6	20.9	26.0	27.8	31.3	33.2	34.7	36.1

It can be seen in the tables that if smart charging is possible at the EVCS, the matching performances can be improved quite significantly. The SC improvement by the smart charging scheme is less significant when the PV system was undersized or oversized, for example the improvements with combined PV-EV sizes (kWp — number of chargers) of 100–20 and 20–100 are lower than with 20–20. As for SS, among the simulated scenarios, with an exception of the scenario with 20 charging ports, the improvement potential is always higher when the PV size was higher. This is due to the fact that more PV generation can be utilized in an oversized PV system to make the system more self-sufficient. That being the case, an EVCS with an oversized PV system is more incentivized to utilize the EV parking time flexibility and deploy smart charging schemes whenever possible. In the scenario with 20 charging

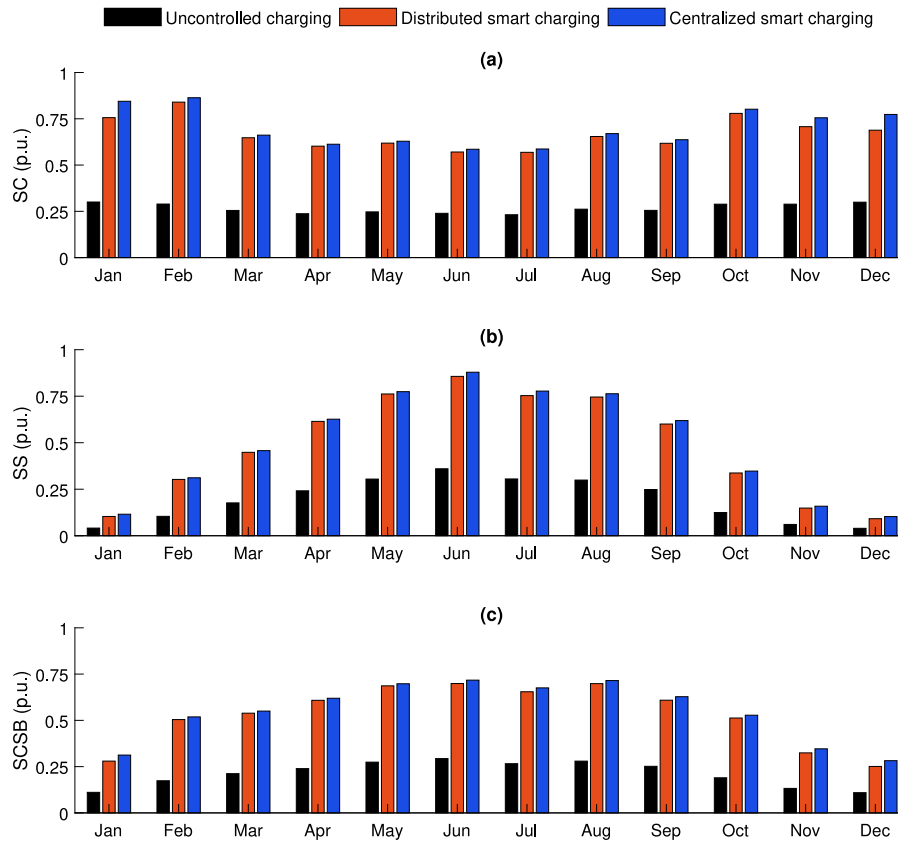


Fig. 11. (a) SC, (b) SS and (c) SCSB in different months in the year: Stockholm case.

Table 3

SS increases in percentage points at the EVCS with varying combined PV-EV sizes with distributed charging (D) and centralized charging (C) compared to uncontrolled charging with a maximum charging power of 11 kW: Stockholm case.

PV system size (kWp)	Number of EV charging ports									
	20		40		60		80		100	
	D	C	D	C	D	C	D	C	D	C
20	29.4	30.7	15.0	15.6	8.5	9.1	5.6	6.2	3.8	4.4
40	36.8	38.8	27.4	28.8	18.7	19.3	12.8	13.4	9.2	9.7
60	38.0	40.8	32.1	34.1	26.2	27.4	20.4	21.1	15.5	15.9
80	37.5	40.2	34.2	36.3	29.6	31.6	25.6	26.7	21.3	21.9
100	36.8	39.3	35.2	37.6	31.6	33.7	28.4	30.1	25.1	26.1

ports, the highest SS improvement is higher in the scenario with 60 kWp PV system than in the scenario with 100 kWp PV system. It is an indication that the smart charging scheme contribute less significantly in improving the SS if the PV system is extremely oversized. This is due to the fact that the SS will be already high with an extremely oversized PV system, thus it leaves less room for the smart charging to improve the SS. As studied in [30], it is more difficult to increase the SC and the SS if they are already high, e.g., increase from 30% to 50% is counted as the same increase as from 50% to 70%, but the latter is more difficult to achieve.

It can also be seen from the tables that the enhancement potentials with the centralized charging was higher than with the distributed charging. However, the difference was not that significant, only between 0.9–3.9 percentage points for the SC and between 0.6–2.8 percentage points for the SS depending on the configuration of PV-EV sizes. Even though the difference was not that significant, it should be noted that a strategy to avoid the avalanche effect is needed for the distributed smart charging scheme to obtain performances close to the

results from the centralized smart charging scheme. For example, in the simulated distributed charging scheme, the strategy was that the PV generation input to the optimization model was scaled down by the number of charging ports. With the centralized charging scheme, the avalanche effect is avoided by design of the centralized smart charging scheme.

### 3.3. Graphical analysis for optimal PV-EV sizing

This section presents the graphical analysis of SC, SS and SCSB which can be a framework or a tool to define the optimal PV-EV sizing in a building or a facility powered by PV systems such as a solar powered workplace charging station. Figs. 12–14 show colormaps of SC, SS and SCSB in different PV-EV sizes for the EVCS in this study with (a) uncontrolled charging, (b) distributed smart charging and (c) centralized smart charging for the Stockholm case. In the figures, the estimation of the SC, the SS and the SCSB between the simulated PV-EV sizes was conducted with a spline interpolation approach. With the colormap framework of Figs. 12 and 13, it is easier to understand that the larger the size of PV system, the lower the SC and the higher the SS; and the larger the number of EV charging ports, the higher the SC and the lower the SS.

As discussed earlier, the SCSB score can be used to define the optimal size of the PV system and number of EV charging ports for a solar powered EVCS. A high SCSB implies that the system is close to being self-sufficient without wasting a large share of local electricity production. In Fig. 14, additional lines following the vertices were added to help pointing out the optimal combined PV-EV sizes. This framework can help one to properly size the PV-EV system more easily. For example, with the uncontrolled/opportunistic charging scheme shown in Fig. 14(a), for an EVCS with 40 charging ports, the optimal PV size is around 50 kWp. PV sizes larger or lower than that would result in lower overall load matching performance. Conversely, in a

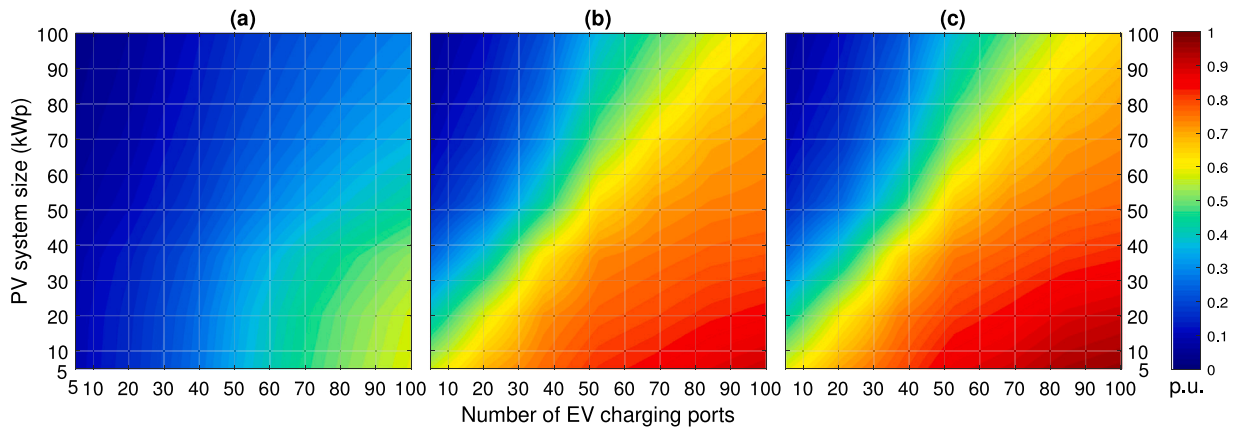


Fig. 12. SC at the workplace charging station for (a) uncontrolled charging, (b) distributed smart charging and (c) centralized smart charging scenarios with different PV sizes and numbers of EV charging ports: Stockholm case.

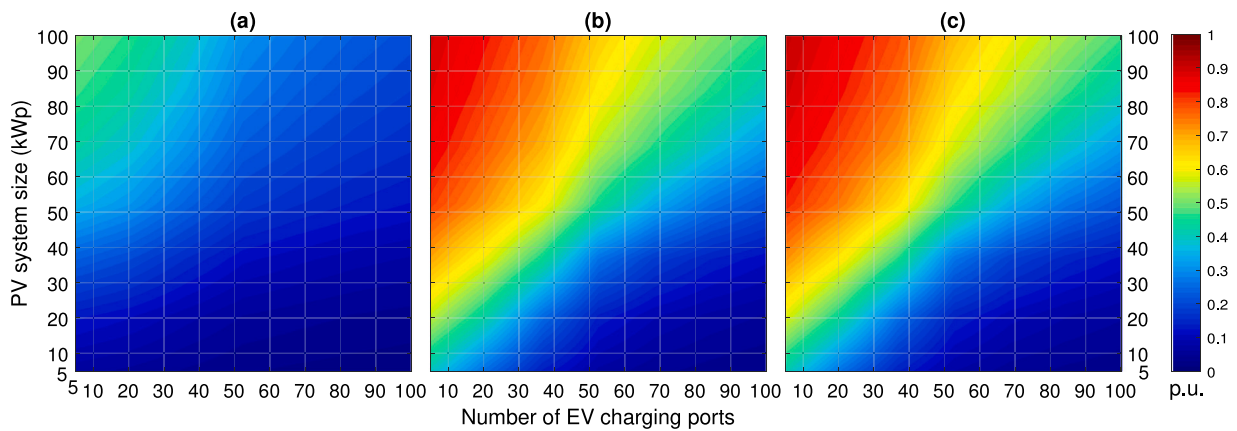


Fig. 13. SS at the workplace charging station for (a) uncontrolled charging, (b) distributed smart charging and (c) centralized smart charging scenarios with different PV sizes and numbers of EV charging ports: Stockholm case.

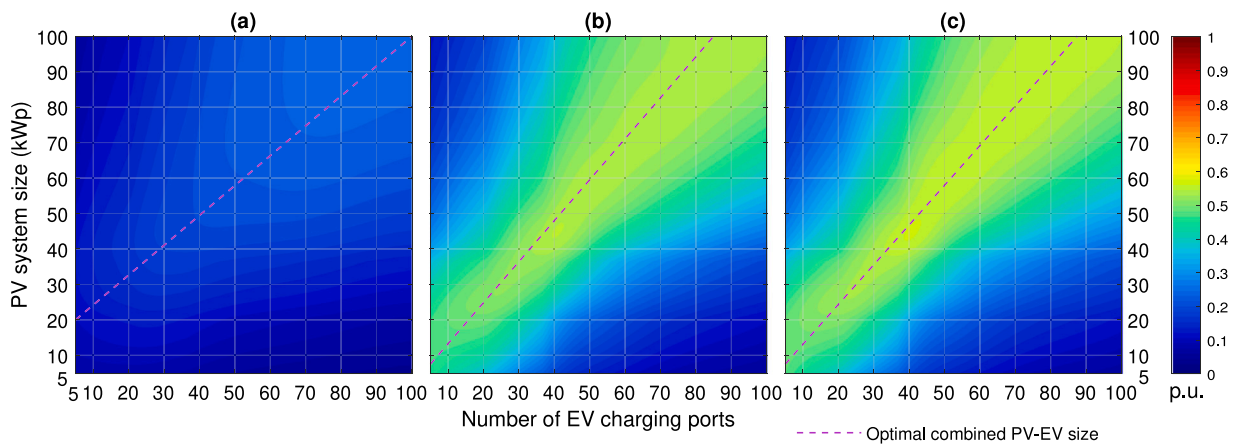


Fig. 14. SCSB at the workplace charging station for (a) uncontrolled charging, (b) distributed smart charging and (c) centralized smart charging scenarios with different PV sizes and numbers of EV charging ports: Stockholm case. The diagonal line represents the estimation of the optimal SCSB in different PV and EV sizes.

similar fashion, the PV system size can be fixed as a basis for determining the number of EV charging ports. For example, for an EVCS with 60 kWp PV systems, the optimal number of charging ports is around 55. More or fewer ports installed at the EVCS will result in lower overall load matching performance. It can be seen that with the uncontrolled/opportunistic charging scheme, the optimal SCSB values are still low and not significantly higher than the non-optimal values.

The smart charging schemes presented in this study can be used to improve the SCSB since the schemes always maximize the self-consumed electricity, which is the numerator in both SC and SS formulas, see Eqs. (10) and (11). It can be seen in Fig. 14(b) and (c), that the SCSB values around the optimum are enhanced significantly with the smart charging schemes. It can also be seen that much larger or smaller sizes of the PV system compared to the number of charging ports still have low SCSB values. Low SCSB is the result of an extremely low value

of either SC or SS or both. That implies that the difference in SCSB performance between a properly-sized and an undersized/oversized PV powered EVCS is highly significant.

By comparing the optimal size lines in Fig. 14(a), (b) and (c), it can be seen that the combined optimal PV-EV sizes with the smart charging schemes are shifted from the ones with the uncontrolled/opportunistic charging scheme, while the results for the distributed and centralized smart charging are almost identical and hardly distinguishable. As it can be seen, compared to the smart charging, the uncontrolled charging scheme requires higher PV size to reach optimum in lower EV size, while it requires lower PV size to reach optimum in higher EV size. This is due to the lower temporal matching in the uncontrolled charging scheme. Thus in order to reach the optimum SCSB, compared to the smart charging scheme, the uncontrolled charging scheme requires higher PV size in a small EVCS to avoid an extremely low SS due to a very small generation. Meanwhile, it requires lower PV size in a large EVCS to avoid an extremely low SC due to massive amount of unconsumed electricity.

With a highly different EV charging load profiles in uncontrolled charging and smart charging scenarios, the relevant stakeholder should take into account the smart charging applicability at the EVCS for PV-EV sizing, since the optimal sizing with and without smart charging will be different. Beside having different combined optimal PV-EV sizes, the optimal SCSB value with the smart charging scheme is significantly higher than the optimal SCSB value with the uncontrolled charging scheme. This implies that the implementation of SCSB enhancements strategies, such as smart charging schemes or BESS deployment, should be strongly considered before defining the optimal combined PV-EV size.

It can also be seen from Fig. 14 that regardless of the charging scenarios, a larger and balanced combined PV-EV size tends to have higher SCSB values than a smaller and balanced combined PV-EV size. This is related to the effect of the aggregation of several PV-load systems where the aggregated SC tends to be higher than a single system SC, as shown in several previous studies, e.g., in [67,72,73].

### 3.3.1. Sensitivity analysis with Hawaii irradiance profile

This section presents the SCSB graphical analysis for an EVCS with the irradiance data from Hawaii in order to show the applicability of the framework for different climatic regions. As a comparison to the Stockholm profile shown in Fig. 14, the SCSB graphical analysis utilizing the Hawaii irradiance data is shown in Fig. 15. It should be noted that the sensitivity analysis focused only on the solar irradiance variable, and the simulation still utilized the Swedish mobility profile. The vehicle specific consumption for Hawaii case was adjusted with Hawaii local temperature.

Compared to Sweden, Hawaii is much closer to the equator where the solar seasonality is significantly lower. Furthermore, the annual PV energy production potential in Hawaii is around 1.8 times higher than in Stockholm [52]. This makes the solar utilization potential in Hawaii generally higher than for the Swedish case. As it can be seen in Fig. 15, the optimal SCSB in Hawaii is higher than the optimal SCSB in Stockholm, especially when the smart charging schemes are deployed. It can also be seen that the optimal SCSB improvement with smart charging schemes in Hawaii is more significant than in Stockholm.

A motivation for investigating the effect of solar irradiance from a different climatic region is that the optimal sizes could differ in different climatic regions due to the difference in solar irradiance profiles. Based on the optimal lines shown in Figs. 14 and 15, the comparison between the optimal combined PV-EV size at the EVCS with uncontrolled and centralized smart charging for the two different irradiance profiles: Stockholm and Hawaii, is shown in Fig. 16. It can be seen from Fig. 16 that, with the uncontrolled charging scheme, the optimal PV size for the same number of EV charging ports in Stockholm is higher than in Hawaii. For example, for an EVCS with 40 EV charging ports, the optimal PV system size is 50 kWp in Stockholm, and 40 in

Hawaii. This is due to the fact that the solar production potential is smaller in Stockholm, so it needs larger PV size to cover the EV load, i.e., to make the SS not too low, and make the SC and SS balanced. For Hawaii, with a higher solar production potential, more EV load is covered with the same PV size. That implies, the highest SCSB potential without smart charging in Hawaii is achieved with lower PV size. It should be noted that the optimal SCSB value in Hawaii is higher than the optimal SCSB value in Stockholm.

The deployment of the smart charging scheme would shift the optimal combined PV-EV sizes both in Stockholm and Hawaii. Beside a more significant SCSB improvement with the smart charging schemes for the Hawaii profile compared to the Stockholm profile, it can also be seen from Fig. 16 that the shift of the optimal combined PV-EV size for the Hawaii profile is more significant than for the Stockholm profile. This is an indication that the consideration of the smart charging schemes are more essential for PV-EV sizing for the Hawaii profile than for the Stockholm profile. Regardless of the superiority of the SCSB scores in Hawaii compared to in Stockholm, the optimal combined PV-EV size with smart charging schemes in both Stockholm and Hawaii are similar.

## 4. Discussion

The results in Section 3 show that the deployment of smart charging at a solar powered workplace charging station could improve the load matching performance. Even though the potential of load matching between PV and EV at the workplaces is comparatively higher than at other places, e.g., at home, the highest potential cannot be achieved with an uncontrolled charging scheme in which the charging is conducted opportunistically. With opportunistic charging behavior, the charging load at workplaces peaks between 08.00–10.00 in the morning, whereas the solar power production peaks between 12.00–13.00 during noon. With smart charging schemes, the daily peak of the charging load can be shifted to the daily solar peak production period, and thereby improve the matching.

It should be noted that the smart charging schemes in this study have a pure technical objective, i.e., flattening the net-load profile, which also implies maximizing the self-consumed electricity. In addition, the schemes also utilized perfect forecast of PV generation. Thus, the SC and SS presented in this study will be best-case approximation or the highest possible performances that can be achieved with a smart charging scheme. The same smart charging scheme with a more realistic forecast, or other smart charging schemes, e.g., schemes with economic objectives, most likely will have lower SC and SS performances. The matching performance assessment using a more realistic forecast and/or different smart charging schemes are left for future studies.

The numerical results in this paper show that the SC can be increased up to 42.6 percentage points with the smart charging scheme for EVCSs in Stockholm. Significant SC improvements in workplaces were also found in previous research. In [27,39], SC improvements by smart charging schemes were up to 49.6 and 52.0 percentage points respectively. In [29,40], the SC improvements were up to 24.5 and 16.5 percentage points respectively. It should be noted that SC improvement variations by smart charging schemes will be highly dependent on several conditions, such as the sizes of the installed PV system and irradiance potentials at the site, the regional user mobility profiles, and the objectives of the smart charging schemes. For example, in [27], the case study was in California where the irradiance is comparatively high, and the main objective of the deployed smart charging scheme was to directly increase the SC. On the other hand, in [29], the case study was in the Netherlands where the irradiance is comparatively lower, and the main objective of the smart charging was to reduce the energy costs. That is why the SC improvements can vary depending on the conditions.

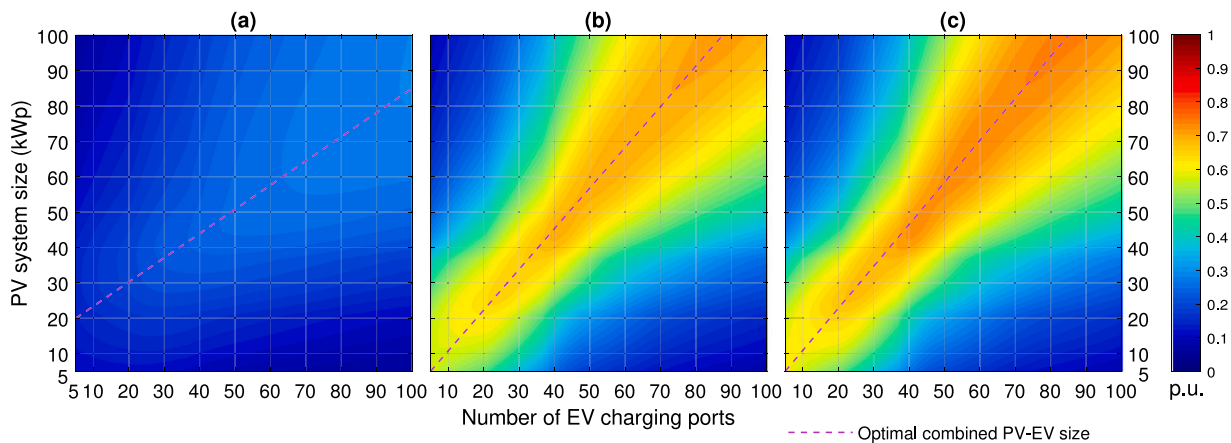


Fig. 15. SCSB at the workplace charging station for (a) uncontrolled charging, (b) distributed smart charging and (c) centralized smart charging scenarios with different PV sizes and numbers of EV charging ports with Hawaii irradiance data. The diagonal line represents the estimation of the optimal SCSB in different PV and EV sizes.

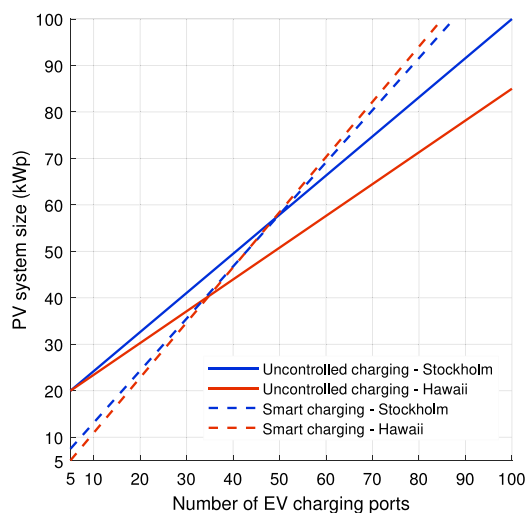


Fig. 16. Optimal PV-EV sizing at the EVCS based on the SCSB values with uncontrolled/opportunistic and centralized smart charging schemes with Stockholm and Hawaii irradiance profiles.

Besides optimal daily operations using smart charging schemes, defining an optimal combined PV-EV size is also important to achieve desired PV utilization performances. Undersized or oversized PV systems would lead to lower overall load matching performances. As discussed earlier, the SCSB score could help relevant stakeholders to properly size the local PV-EV system configuration, or PV-load matching in general, as the SCSB score conveys the balance between the SC and SS. This implies that a system with high SCSB will be close to being self-sufficient without wasting a large share of PV production. Apart for the EVCS owner, a high SCSB performance will also benefit the power grid operator since grid interaction is minimized. The SCSB formulation can also be modified with different weighting factors for each of SC and SS. This might be needed when either of SC or SS is more important than the other in specific case studies, but it was not the case for this paper.

A graphical-based framework to define the optimal size based on SCSB was presented and proposed in this study. This framework can help relevant stakeholders to define a proper size of a PV-EV system, or answer important questions when designing a PV-EV system for an EVCS, such as how much PV systems should be installed if the EVCS has a certain number of charging ports? Or conversely, how many charging ports should be installed if one can install a certain kWp PV system at the area?

The results show that, beside significantly enhancing the load matching performance, the smart charging would also shift the optimal combined PV-EV sizes. This is due to the fact that the uncontrolled and smart charging schemes have different generation-load temporal matching profiles. Thereby, it is important to take into account the smart charging scheme applicability at the EVCS, since the optimal sizing results with and without smart charging will be different. Considering significantly higher optimal SCSB value with the smart charging compared to the one with the uncontrolled charging, the relevant stakeholder should strongly consider deploying smart charging schemes at the EVCS whenever possible.

The sensitivity analysis utilizing different solar irradiance profiles was conducted in this study in order to strengthen the universality claim of this framework. The framework was used to define the optimal PV-EV sizing at the workplace EVCS with two different irradiance profiles in two different climatic regions: Hawaii and Stockholm. Due to the higher solar energy production potentials and lower solar seasonality, the SCSB performance for Hawaii is higher than the one for Stockholm. The results also show that the optimal combined PV-EV sizing profiles for Hawaii and Stockholm, are significantly different with the uncontrolled charging scenarios, but similar with the smart charging scenarios. Future studies should compare the optimal combined PV-EV sizing, both with uncontrolled and smart charging schemes, in more climatic regions and with representative mobility profiles.

It should be noted that, the optimal sizing framework based on SCSB will result in a pure technical optimum. The proposed framework does not consider other aspects such as economic and environmental aspects. As discussed earlier in Section 1.1, most studies have focused on economic objectives, and not technical ones in defining optimal PV and EV sizes. It is worth bearing in mind that the cost-optimal framework will be subject to local policies and regulations. Variables such as electricity prices, LCOE, feed in tariffs, tax and subsidy related to RES and CO<sub>2</sub> emissions, PV-grid power exchange permission are among factors which are most likely varying between regions and countries [52]. That being the case, the cost optimal sizing framework will most likely require different formulation for different case studies, thus less suitable to be used a benchmark. On the other hand, the SC and SS formulation are universal for any local PV systems which makes the optimal PV-load sizing based on SCSB a simpler and more universal framework to be a benchmark.

Despite big interests from the EVCS owner in cost-optimal sizing, the SCSB-optimal sizing will still be highly relevant as technical and economic benefits are often strongly correlated [13]. The simple optimal SCSB framework can be used as a consideration before going to a cost and revenue calculation in the detailed feasibility study. Future studies on cost-optimal sizing of local PV systems is encouraged to include SCSB-optimal sizing as the benchmark for comparison.

Beside the benefits for the EVCS owner, an SCSB-optimal PV-EV sizes and operation in the solar powered EVCS will most likely benefit other relevant stakeholders. For example, the power grid operators will benefit as the grid interaction of the newly integrated solar powered EVCS will be minimal. In such conditions, an expensive and time-consuming grid reinforcement can be avoided. Furthermore, the application of the proposed optimal framework in the real world systems can contribute to achieve an optimal RES utilization, which consequently reduces the energy costs as well as the GHG emissions. In other words, it can contribute to a more sustainable energy system.

As discussed earlier, the SCSB framework can be used universally for any RES powered buildings or infrastructures to define a proper generation-load system size. Therefore, future studies using the same framework for different parts of the built environment and generation-load technologies other than PV-EV are recommended. Some examples of EVCS at different parts of the built environment are EVCS at residential areas, commercial buildings such as malls, or a cluster area combining residential, workplace and commercial buildings. Some examples of other generation-load technologies that can utilize the framework are the sizing of PV-heat pump, wind-EV, wind-heat pump.

It was shown in this paper that DSM strategies such as smart charging can enhance the overall SCSB performance. It is expected that the storage deployment will also improve the SCSB and alter the optimal combined PV-EV sizes as it is with DSM strategies. Studies on optimal PV-EV sizing, or generation-load sizing in general, based on SCSB using different storage sizes are also recommended for future works.

Beside optimal local generation-load sizing, the correlation between power grid performances and the SCSB measure is interesting for future studies. In such studies, it should be noted that, not only the newly integrated loads, e.g., EVs or heat pumps, but also the existing load in the distribution system, e.g., existing residential and office building loads, should be taken into account into the SCSB calculation.

## 5. Conclusion

This paper presents a study on optimal sizing framework for PV system and EV charging ports at workplaces with solar powered EVCS. A case study for Swedish conditions was simulated and a sensitivity analysis using Hawaii irradiance profile was conducted. A novel score based on harmonic mean between SC and SS was proposed to define the optimal combined PV-EV size. The score, which is called SCSB, conveys the balance between the SC and the SS. A system with high SCSB will be close to being self-sufficient (high SS) without curtailing or exporting a large share of local generation (high SC). In addition to optimal sizing, this paper also assessed the performance enhancement potential using smart charging schemes at the workplace EVCS. The smart charging schemes in this study was intended to flatten the net-load profile, which implies maximizing the self-consumed electricity.

Several conclusions can be drawn from this study:

1. The deployment of the smart charging can significantly improve the PV-EV load matching at the PV powered EVCS, by up to 42.6 percentage points in SC and up to 40.8 percentage points in SS.
2. The centralized smart charging scheme provides a slightly higher load matching performance compared to the distributed smart charging scheme, i.e., up to 1.9 percentage points difference in SC and 2.8 percentage points difference in SS.
3. The optimal framework based on the novel metric SCSB proposed in this study, can be used to define how large PV systems that should be installed if there are a certain number of charging ports, and vice versa, how much charging ports should be installed if there is a certain kWp PV system integrated on-site.
4. Regardless of the charging strategies, the SCSB performance of the PV powered EVCS tends to be higher in a larger combined PV-EV size compared to in a smaller size.

5. The deployment of the smart charging scheme will shift the optimal combined PV-EV sizes from the ones in the uncontrolled charging scheme.

Even though this paper presented a specific case study of PV-EV sizing at workplace EVCS, the proposed framework can be used to define a proper generation-load system size for other parts of the built environment and/or technologies in future studies. For examples, PV-EV sizing at residential areas or commercial buildings such as malls, and/or sizing of PV-heat pump, wind-EV or wind-heat pump at relevant locations. Due to its simplicity and universality for RES powered buildings or infrastructures, the sizing framework based on SCSB metric presented in this study can be used as a benchmark framework.

## CRedit authorship contribution statement

**Reza Fachrizal:** Conceptualization, Methodology, Software, Data curation, Visualization, Formal analysis, Funding acquisition, Writing - original draft. **Mahmoud Shepero:** Conceptualization, Methodology, Funding acquisition, Writing - reviewing & editing. **Magnus Åberg:** Conceptualization, Writing - Reviewing and Editing. **Joakim Munkhammar:** Supervision, Conceptualization, Funding acquisition, Writing - reviewing & editing.

## Declaration of competing interest

The authors declare that they have no known competing financial interests or personal relationships that could have appeared to influence the work reported in this paper.

## Acknowledgment

This study was conducted as part of the research project 'Smart charging strategies and optimal PV-EV sizing to increase the combined PV-EV hosting capacity in the distribution grid', funded through Swe-GRIDS, by the Swedish Energy Agency. This work also forms part of the Swedish strategic research programme StandUp for Energy.

## References

- [1] Intergovernmental Panel on Climate Change (IPCC). Climate change 2014 mitigation of climate change. Tech. Rep., 2014, URL <https://www.ipcc.ch/report/ar5/wg3/>.
- [2] International Energy Agency. Global energy & CO 2 status report. Tech. Rep., 2017, URL <https://www.iea.org/publications/freepublications/publication/GECO2017.pdf>.
- [3] Tran M, Banister D, Bishop JD, McCulloch MD. Realizing the electric-vehicle revolution. *Nat Clim Chang* 2012;2(5):328–33. <http://dx.doi.org/10.1038/nclimate1429>.
- [4] Luthander R, Shepero M, Munkhammar J, Widén J. Photovoltaics and opportunistic electric vehicle charging in the power system – a case study on a Swedish distribution grid. *IET Renew Power Gener* 2019;13(5):710–6. <http://dx.doi.org/10.1049/iet-rpg.2018.5082>.
- [5] Khalid MR, Alam MS, Sarwar A, Asghar MSJ. A comprehensive review on electric vehicles charging infrastructures and their impacts on power-quality of the utility grid. *ETransportation* 2019;1:100006. <http://dx.doi.org/10.1016/j.etrans.2019.100006>.
- [6] Denholm P, O'Connell M, Brinkman G, Jorgenson J. Overgeneration from solar energy in california. a field guide to the duck chart. Tech. Rep., (November). National Renewable Energy Laboratory (NREL); 2015. <http://dx.doi.org/10.2172/1226167>.
- [7] Guo C, Zhu K, Chen C, Xiao X. Characteristics and effect laws of the large-scale electric vehicle's charging load. *ETransportation* 2020;3:100049. <http://dx.doi.org/10.1016/j.etrans.2020.100049>.
- [8] Johansson S, Persson J, Lazarou S, Theocharis A. Investigation of the impact of large-scale integration of electric vehicles for a Swedish distribution network. *Energies* 2019;12(24). <http://dx.doi.org/10.3390/en12244717>.
- [9] Dixon J, Bell K. Electric vehicles: battery capacity, charger power, access to charging and the impacts on distribution networks. *ETransportation* 2020;4:100059. <http://dx.doi.org/10.1016/j.etrans.2020.100059>.

- [10] Uski S, Forssén K, Shemeikka J. Sensitivity assessment of microgrid investment options to guarantee reliability of power supply in rural networks as an alternative to underground cabling. *Energies* 2018;11(10). <http://dx.doi.org/10.3390/en11102831>.
- [11] Bertsch V, Geldermann J, Lühn T. What drives the profitability of household PV investments, self-consumption and self-sufficiency? *Appl Energy* 2017;204:1–15. <http://dx.doi.org/10.1016/j.apenergy.2017.06.055>.
- [12] Amjad M, Ahmad A, Rehmani MH, Umer T. A review of EVs charging: From the perspective of energy optimization, optimization approaches, and charging techniques. *Transp Res D* 2018;62(March):386–417. <http://dx.doi.org/10.1016/j.trd.2018.03.006>.
- [13] Fachrizal R, Shepero M, van der Meer D, Munkhammar J, Widén J. Smart charging of electric vehicles considering photovoltaic power production and electricity consumption: a review. *ETransportation* 2020;4:100056. <http://dx.doi.org/10.1016/j.etrans.2020.100056>.
- [14] Ramadhani UH, Fachrizal R, Shepero M, Munkhammar J, Wid J. Probabilistic load flow analysis of electric vehicle smart charging in unbalanced LV distribution systems with residential photovoltaic generation. *Sustain Cities Soc* 2021;72. <http://dx.doi.org/10.1016/j.scs.2021.103043>.
- [15] Felipe A, Borray C, Merino J, Torres E, Garcés A, Mazón J. Centralised coordination of EVs charging and PV active power curtailment over multiple aggregators in low voltage networks. *Sustain Energy Grids Netw* 2021;27:100470. <http://dx.doi.org/10.1016/j.segan.2021.100470>.
- [16] Ye R, Huang X, Chen Z, Ji Z. A hybrid charging management strategy for solving the under-voltage problem caused by large-scale EV fast charging. *Sustain Energy Grids Netw* 2021;27:100508. <http://dx.doi.org/10.1016/j.segan.2021.100508>.
- [17] Edmunds C, Galloway S, Dixon J, Bukhsh W, Elders I. Hosting capacity assessment of heat pumps and optimised electric vehicle charging on low voltage networks. *Appl Energy* 2021;298(June):117093. <http://dx.doi.org/10.1016/j.apenergy.2021.117093>.
- [18] Fachrizal R, Ramadhani UH, Munkhammar J, Widén J. Combined PV – EV hosting capacity assessment for a residential LV distribution grid with smart EV charging and PV curtailment. *Sustain Energy Grids Netw* 2021;26:100445. <http://dx.doi.org/10.1016/j.segan.2021.100445>.
- [19] Da Silva EC, Melgar-Dominguez OD, Romero R. Simultaneous distributed generation and electric vehicles hosting capacity assessment in electric distribution systems. *IEEE Access* 2021;9:110927–39. <http://dx.doi.org/10.1109/ACCESS.2021.3102684>.
- [20] Heinisch V, Göransson L, Erlandsson R, Hodel H, Johnsson F, Odenberger M. Smart electric vehicle charging strategies for sectoral coupling in a city energy system. *Appl Energy* 2021;288(January). <http://dx.doi.org/10.1016/j.apenergy.2021.116640>.
- [21] Saber AY, Venayagamoorthy GK. Plug-in vehicles and renewable energy sources for cost and emission reductions. *IEEE Trans Ind Electron* 2011;58(4):1229–38. <http://dx.doi.org/10.1109/TIE.2010.2047828>.
- [22] Li D, Zouma A, Liao JT, Yang HT. An energy management strategy with renewable energy and energy storage system for a large electric vehicle charging station. *ETransportation* 2020;6:100076. <http://dx.doi.org/10.1016/j.etrans.2020.100076>.
- [23] Schram WL, Aghaie H, Lampropoulos I, Sark WGJHMV. Insights on the capacity value of photovoltaics, community batteries and electric vehicles. *Sustain Energy Grids Netw* 2021;26:100421. <http://dx.doi.org/10.1016/j.segan.2020.100421>.
- [24] Mohammad A, Zamora R, Lie TT. Integration of electric vehicles in the distribution network : A review of PV based electric vehicle modelling. *Energies* 2020;13. <http://dx.doi.org/10.3390/en13174541>.
- [25] Pareschi G, Küng L, Georges G, Boulouchos K. Are travel surveys a good basis for EV models? Validation of simulated charging profiles against empirical data. *Appl Energy* 2020;275(June):115318. <http://dx.doi.org/10.1016/j.apenergy.2020.115318>.
- [26] Pasaoglu G, Fiorello D, Martino A, Zani L, Zubaryeva A, Thiel C. Travel patterns and the potential use of electric cars - results from a direct survey in six European countries. *Technol Forecast Soc Change* 2014;87:51–9. <http://dx.doi.org/10.1016/j.techfore.2013.10.018>.
- [27] Zhang T, Chu CC, Gadh R. A two-tier energy management system for smart electric vehicle charging in UCLA: A solar-to-vehicle (S2V) case study. In: *IEEE PES innov. smart grid technol. conf. eur.*. Melbourne, Australia: IEEE; 2016, p. 288–93. <http://dx.doi.org/10.1109/ISGT-Asia.2016.7796400>.
- [28] Chandra Mouli GR, Bauer P, Zeman M. System design for a solar powered electric vehicle charging station for workplaces. *Appl Energy* 2016;168(2016):434–43. <http://dx.doi.org/10.1016/j.apenergy.2016.01.110>.
- [29] Van der Meer D, Mouli GRC, Mouli GME, Elizondo LR, Bauer P. Energy management system with PV power forecast to optimally charge EVs at the workplace. *IEEE Trans Ind Inf* 2018;14(1):311–20. <http://dx.doi.org/10.1109/TII.2016.2634624>.
- [30] Luthander R, Widén J, Nilsson D, Palm J. Photovoltaic self-consumption in buildings: A review. *Appl Energy* 2015;142:80–94. <http://dx.doi.org/10.1016/j.apenergy.2014.12.028>.
- [31] Luthander R, Nilsson AM, Widén J, Åberg M. Graphical analysis of photovoltaic generation and load matching in buildings: A novel way of studying self-consumption and self-sufficiency. *Appl Energy* 2019;250(November 2018):748–59. <http://dx.doi.org/10.1016/j.apenergy.2019.05.058>.
- [32] Van den Berg MA, Lampropoulos I, Alskaf TA. Impact of electric vehicles charging demand on distribution transformers in an office area and determination of flexibility potential. *Sustain Energy Grids Netw* 2021;26:100452. <http://dx.doi.org/10.1016/j.segan.2021.100452>.
- [33] Roselli C, Sasso M. Integration between electric vehicle charging and PV system to increase self-consumption of an office application. *Energy Convers Manag* 2016;130:130–40. <http://dx.doi.org/10.1016/j.enconman.2016.10.040>.
- [34] Ghotge R, van Wijk A, Lukszo Z. Off-grid solar charging of electric vehicles at long-term parking locations. *Energy* 2021;227. <http://dx.doi.org/10.1016/j.energy.2021.120356>.
- [35] Goli P, Shireen W. PV powered smart charging station for PHEVs. *Renew Energy* 2014;66:280–7. <http://dx.doi.org/10.1016/j.renene.2013.11.066>.
- [36] Mohamed A, Salehi V, Ma T, Mohammed O. Real-time energy management algorithm for plug-in hybrid electric vehicle charging parks involving sustainable energy. *IEEE Trans Sustain Energy* 2014;5(2):577–86. <http://dx.doi.org/10.1109/TSTE.2013.2278544>.
- [37] Yao L, Damiran Z, Lim WH. Optimal charging and discharging scheduling for electric vehicles in a parking station with photovoltaic system and energy storage system. *Energies* 2017;10(4). <http://dx.doi.org/10.3390/en10040550>.
- [38] Moghaddam V, Ahmad I, Habibi D, Masoum MA. Dispatch management of portable charging stations in electric vehicle networks. *ETransportation* 2021;8:100112. <http://dx.doi.org/10.1016/j.etrans.2021.100112>.
- [39] Shang Y, Yu H, Niu S, Shao Z, Jian L. Cyber-physical co-modeling and optimal energy dispatching within internet of smart charging points for vehicle-to-grid operation. *Appl Energy* 2021;303(June):117595. <http://dx.doi.org/10.1016/j.apenergy.2021.117595>.
- [40] Dorokhova M, Martinson Y, Ballif C, Wyrsh N. Deep reinforcement learning control of electric vehicle charging in the presence of photovoltaic generation. *Appl Energy* 2021;301(August):117504. <http://dx.doi.org/10.1016/j.apenergy.2021.117504>.
- [41] Litjens GBMA, Kausika BB, Worrell E, Sark WGJHMV. A spatio-temporal city-scale assessment of residential photovoltaic power integration scenarios. *Sol Energy* 2018;174(July):1185–97. <http://dx.doi.org/10.1016/j.solener.2018.09.055>.
- [42] Hernández JC, Sanchez-sutil F, Muñoz rodríguez FJ, Baier CR. Optimal sizing and management strategy for PV household-prosumers with self-consumption / sufficiency enhancement and provision of frequency containment reserve. *Appl Energy* 2020;277(July):115529. <http://dx.doi.org/10.1016/j.apenergy.2020.115529>.
- [43] Gomez-gonzalez M, Hernandez JC, Vera D, Jurado F. Optimal sizing and power schedule in PV household-prosumers for improving PV self-consumption and providing frequency containment reserve. *Energy* 2020;191:116554. <http://dx.doi.org/10.1016/j.energy.2019.116554>.
- [44] Wang C, Tian L, Zhang F, Cheng L. Optimal sizing of photovoltaic and battery energy storage of electric vehicle charging station based on two-part electricity pricing. In: *2020 IEEE sustain. power energy conf.*, Chengdu, China. 2020. p. 1379–84.
- [45] Yan D, Ma C. Optimal sizing of a PV based electric vehicle charging station under uncertainties. In: *IECON 2019 - 45th annu. conf. IEEE ind. electron. soc.*. Lisbon, Portugal: IEEE; 2019, p. 4310–5.
- [46] Kouka K, Masmoudi A, Abdelkafi A, Krichen L. Dynamic energy management of an electric vehicle charging station using photovoltaic power. *Sustain Energy Grids Netw* 2020;24:100402. <http://dx.doi.org/10.1016/j.segan.2020.100402>.
- [47] Quoc D, Yang Z, Trinh H. Determining the size of PHEV charging stations powered by commercial grid-integrated PV systems considering reactive power support. *Appl Energy* 2020;183(2016):160–9. <http://dx.doi.org/10.1016/j.apenergy.2016.08.168>.
- [48] Liu G, Chinthavali MS, Debnath S, Tomsovic K. Optimal sizing of an electric vehicle charging station with integration of PV and energy storage. In: *2021 IEEE power energy soc. innov. smart grid technol. conf.* 2021. p. 7–11.
- [49] Mirzaei MJ, Kazemi A. A dynamic approach to optimal planning of electric vehicle parking lots. *Sustain Energy Grids Netw* 2020;24:100404. <http://dx.doi.org/10.1016/j.segan.2020.100404>.
- [50] Campaña M, Inga E, Cárdenas J. Optimal sizing of electric vehicle charging stations considering urban traffic flow for smart cities. *Energies* 2021;14(16):1–16. <http://dx.doi.org/10.3390/en14164933>.
- [51] Gough M, Lotfi M, Santos F, Helena M, Espassandim D, Shafie-khah M, Catal PS. Rooftop photovoltaic parking lots to support electric vehicles charging : A comprehensive survey. *Int J Electr Power Energy Syst* 2021;133(November 2020). <http://dx.doi.org/10.1016/j.ijepes.2021.107274>.
- [52] Energy Sector Management Assistance Program (ESMAP). Global photovoltaic power potential by country. *Tech. Rep.*, (June). The World Bank; 2020. <http://dx.doi.org/10.1596/34102>.
- [53] Salom J, Marszal AJ, Widén J, Candanedo J, Lindberg KB. Analysis of load match and grid interaction indicators in net zero energy buildings with simulated and monitored data. *Appl Energy* 2014;136:119–31. <http://dx.doi.org/10.1016/j.apenergy.2014.09.018>.
- [54] Cao S, Hasan A, Sirén K. On-site energy matching indices for buildings with energy conversion, storage and hybrid grid connections. *Energy Build* 2013;64:423–38. <http://dx.doi.org/10.1016/j.enbuild.2013.05.030>.

- [55] Matallanas E, Solórzano J, Castillo-Cagigal M, Navarro I, Caamaño Martín E, Egido MA, Gutiérrez A. Electrical energy balance contest in solar decathlon europe 2012. *Energy Build* 2014;83:36–43. <http://dx.doi.org/10.1016/j.enbuild.2014.03.076>.
- [56] Chabaud A, Eynard J, Grieu S. A new approach to energy resources management in a grid-connected building equipped with energy production and storage systems: A case study in the south of France. *Energy Build*. 2015;99:9–31. <http://dx.doi.org/10.1016/j.enbuild.2015.04.007>.
- [57] Chabaud A, Eynard J, Grieu S. A rule-based strategy to the predictive management of a grid-connected residential building in southern France. *Sustain Cities Soc* 2017;30:18–36. <http://dx.doi.org/10.1016/j.scs.2016.12.016>.
- [58] Meteororm. 2008, URL <http://meteororm.com>.
- [59] Sengupta M, Andreas A. Oahu solar measurement grid (1-year archive):1-second solar irradiance; Oahu, Hawaii (Data). Tech. Rep. DA-5500-56506, National Renewable Energy Laboratory (NREL); 2010, URL <http://dx.doi.org/10.5439/1052451>.
- [60] Munkhammar J, Grahn P, Widén J. Quantifying self-consumption of on-site photovoltaic power generation in households with electric vehicle home charging. *Sol Energy* 2013;97:208–16. <http://dx.doi.org/10.1016/j.solener.2013.08.015>.
- [61] Vattenfall solcellspaket. 2021, URL <https://www.vattenfall.se/solceller/solcellspaket/>.
- [62] RES 2005 – 2006 The national travel survey. Tech. Rep. No. 2007:19, Swedish Institute for Transport and Communications Analysis, SIKa; 2007, URL [www.sika-institute.se](http://www.sika-institute.se).
- [63] Swedish meteorology and hydrology institute. 2018, [Online, accessed March 2021] URL <https://www.smhi.se/data/meteorologi/ladda-ner-meteorologiska-observationer#param=airtemperatureInstant,stations=all,stationid=98735>.
- [64] Kambly KR, Bradley TH. Estimating the HVAC energy consumption of plug-in electric vehicles. *J Power Sources* 2014;259:117–24. <http://dx.doi.org/10.1016/j.jpowsour.2014.02.033>.
- [65] Mathieu L. Recharge EU: How many charge points will europe and its member states need in the 2020s. Tech. Rep., Brussels, Belgium: Transport & Environment; 2020, URL <https://www.transportenvironment.org/publications/recharge-eu-how-many-charge-points-will-eu-countries-need-2030>.
- [66] Sears J, Roberts D, Glitman K. A comparison of electric vehicle level 1 and level 2 charging efficiency. In: 2014 IEEE conf. technol. sustain. sustech 2014. IEEE; 2014, p. 255–8. <http://dx.doi.org/10.1109/SusTech.2014.7046253>.
- [67] Fachrizal R, Munkhammar J. Improved photovoltaic self-consumption in residential buildings with distributed and centralized smart charging of electric vehicles. *Energies* 2020;13(5). <http://dx.doi.org/10.3390/en13051153>.
- [68] Kühnbach M, Stute J, Klingler AL. Impacts of avalanche effects of price-optimized electric vehicle charging - does demand response make it worse? *Energy Strateg Rev* 2021;34:100608. <http://dx.doi.org/10.1016/j.esr.2020.100608>.
- [69] Jahangir H, Golkar MA, Ahmadian A, Elkamel A. Why electric vehicles? In: *Electric vehicle in energy system: modelling, integration, analysis and optimization*. Cham, Switzerland: Springer; 2020.
- [70] Agarwal B. *Basic statistics*. sixth ed.. Cambridge, Massachusetts, U.S.: New Age International Publishers; 2012.
- [71] Murphy KP. *Machine learning: A probabilistic perspective*. Cambridge, Massachusetts, U.S.: MIT Press; 2012, <http://dx.doi.org/10.1111/j.1468-0394.1988.tb00341.x>.
- [72] Luthander R, Lingfors D, Widén J. Large-scale integration of photovoltaic power in a distribution grid using power curtailment and energy storage. *Sol Energy* 2017;155:1319–25. <http://dx.doi.org/10.1016/j.solener.2017.07.083>.
- [73] Huang P, Lovati M, Zhang X, Bales C. A coordinated control to improve performance for a building cluster with energy storage, electric vehicles, and energy sharing considered. *Appl Energy* 2020;268(March):114983. <http://dx.doi.org/10.1016/j.apenergy.2020.114983>.